

Coordination Chemistry

The Synthesis, Characterization and Dehydrogenation of Sigma-Complexes of BN-Cyclohexanes

Amit Kumar,^[a] Jacob S. A. Ishibashi,^[b] Thomas N. Hooper,^[a] Tanya C. Mikulas,^[c] David A. Dixon,^[c] Shih-Yuan Liu,^{*,[b]} and Andrew S. Weller^{*,[a]}

Dedicated to Professor Larry Sneddon in recognition of his outstanding contributions to the transition metal chemistry of boron

Abstract: The coordination chemistry of the 1,2-BN-cyclohexanes 2,2-R₂-1,2-B,N-C₄H₁₀ (R₂ = HH, MeH, Me₂) with Ir and Rh metal fragments has been studied. This led to the solution (NMR spectroscopy) and solid-state (X-ray diffraction) characterization of [Ir(PCy₃)₂(H)₂(η²η²-H₂BNR₂C₄H₈)] [BAR^F₄] (NR₂ = NH₂, NMeH) and [Rh(iPr₂PCH₂CH₂CH₂PiPr₂)(η²η²-H₂BNR₂C₄H₈)] [BAR^F₄] (NR₂ = NH₂, NMeH, NMe₂). For NR₂ = NH₂ subsequent metal-promoted, dehydrocoupling shows the eventual formation of the cyclic tricyclic borazine [BNC₄H₈]₃, via amino-borane and, tentatively characterized using DFT/GIAO chemical shift calculations, cycloborazane intermedi-

ates. For NR₂ = NMeH the final product is the cyclic amino-borane HBNMeC₄H₈. The mechanism of dehydrogenation of 2,2-H,Me-1,2-B,N-C₄H₁₀ using the {Rh(iPr₂PCH₂CH₂CH₂PiPr₂)}⁺ catalyst has been probed. Catalytic experiments indicate the rapid formation of a dimeric species, [Rh₂(iPr₂PCH₂CH₂CH₂PiPr₂)₂H₂][BAR^F₄]. Using the initial rate method starting from this dimer, a first-order relationship to [amine-borane], but half-order to [Rh] is established, which is suggested to be due to a rapid dimer–monomer equilibrium operating.

Introduction

The metal-catalysed dehydrocoupling of amine-boranes is an important methodology for the production of polyaminoboranes that are isoelectronic analogues of polyolefins. The parent compound H₃B-NH₃ is also of significant interest with regard to its ability to act as a chemical hydrogen store, due to its high weight %H (19.6%) and the ability to release H₂ for subsequent utilization in a fuel cell.^[1–6] Such catalytic methodologies offer control of kinetics, product distributions and the temperatures of H₂ loss when compared to simple thermal activation.

Cyclic amine-boranes^[7] such as 1,2-BN cyclohexanes (e.g., **1–3**, Scheme 1 A),^[8,9] BN-methylcyclopentane (**I**, Scheme 1 C)^[10,11]

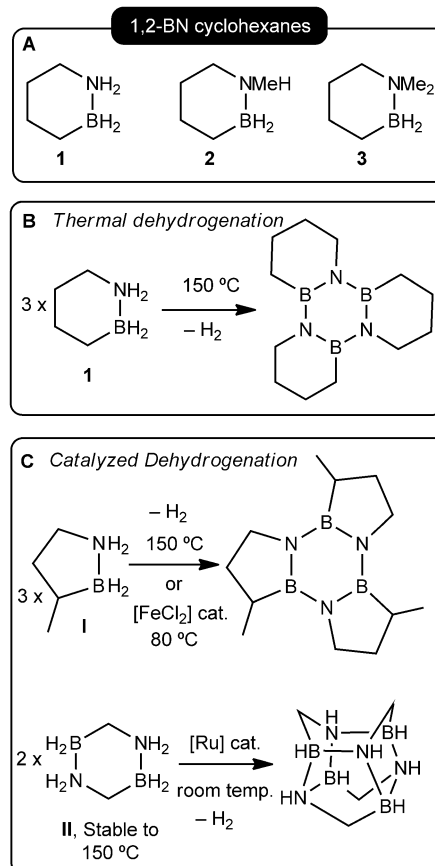
[a] A. Kumar, Dr. T. N. Hooper, Prof. A. S. Weller
Department of Chemistry, University of Oxford
Mansfield Road, Oxford, OX1 3TA (UK)
E-mail: andrew.weller@chem.ox.ac.uk

[b] J. S. A. Ishibashi, Prof. S.-Y. Liu
Department of Chemistry, Boston College
Chestnut Hill, Massachusetts, 02467-3860 (USA)
E-mail: shihyuan.liu@bc.edu

[c] T. C. Mikulas, Prof. D. A. Dixon
Department of Chemistry, The University of Alabama
Tuscaloosa, Alabama 35487-0336 (USA)

Supporting information for this article is available on the WWW under <http://dx.doi.org/10.1002/chem.201502986>.

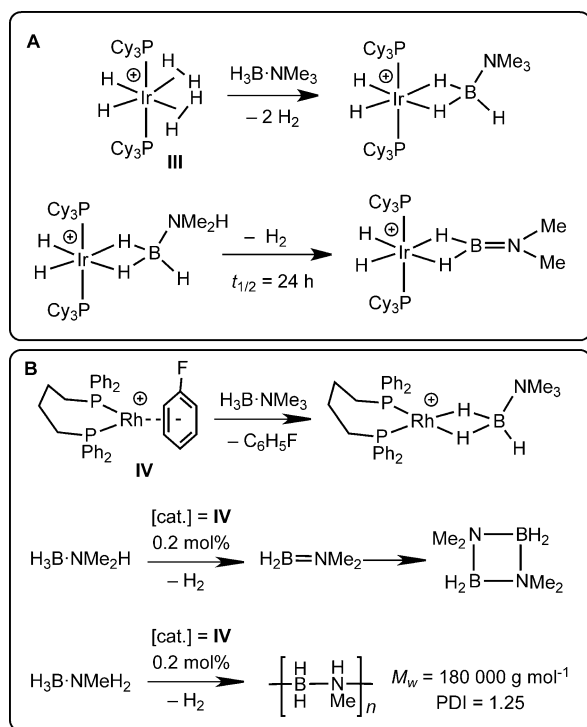
© 2015 The Authors. Published by Wiley-VCH Verlag GmbH & Co. KGaA. This is an open access article under the terms of the Creative Commons Attribution License, which permits use, distribution and reproduction in any medium, provided the original work is properly cited.



Scheme 1. Cyclic BN compounds and their subsequent dehydrogenation.

and bis-BN cyclohexane (II, Scheme 1C)^[12] are attractive candidates for H₂ storage applications as they release H₂ on heating to form well-defined molecular species (Scheme 1B and C) for which viable regeneration routes can be developed.^[8,10] H₂ loss that is promoted by a transition-metal-based catalyst offers a significant reduction in the temperature of release (Scheme 1C), and heterogeneous (e.g., FeCl₂ precatalyst)^[10] and homogeneous (Ru-based)^[12] systems have been developed for use with cyclic amine-boranes. Related B-substituted acyclic systems also undergo dehydrogenation using CoCl₂ as a precatalyst to form B-substituted borazines.^[13] However, the nature of likely intermediates in these dehydrocoupling processes have not been determined, either because of the thermal conditions required in the absence of catalyst (e.g., 150 °C), the generally heterogeneous nature of the catalyst system, or lack of observable intermediates in homogeneous systems (Ru catalysts).

Sigma-amine-borane complexes^[14,15] are key intermediates in inner-sphere transition-metal-catalysed amine-borane dehydrocoupling;^[1] and they are now well-established in terms of both fundamental coordination chemistry, B–H/N–H activation processes and, increasingly, B–N coupling events.^[1] Of particular relevance to this work are those complexes that arise from interaction of either an {Ir(PCy₃)₂(H)₂}⁺^[16–18] or a {Rh(chelating-diphosphine)}⁺^[19,20] fragment with amine-boranes. The former promotes dehydrogenation of the coordinated amine-boranes rather slowly, but leads to the isolation of metal bound intermediates (Scheme 2A), while the latter promotes dehydrogenation much more rapidly, leading to the use of low catalyst loadings (e.g., Scheme 2B).



Scheme 2. Well-defined H₃B-NR₃ sigma complexes (R₃ = Me_xH_{3-x}; x = 1–3) and catalyzed dehydrocoupling. [BAR^F₄][–] anions are not shown.

As far as we are aware, the coordination chemistry of cyclic amine-boranes has not been explored, although rhodium sigma-complexes of the cyclic amine-borane oligomers [H₂BNMe₂]₂^[21] and [H₂BNMeH]₃^[22] have been described. The dehydrogenative cyclization of diamineboranes has been reported to form cyclic diamineboranes using a [Ru(PCy₃)₂(H)₂(H)₂] catalyst;^[23,24] the metal-catalysed dehydrocoupling of base-stabilised diborane(6) [H₂B(hpp)]₂ to give [HB(hpp)]₂ (hpp = 1,3,4,6,7,8-hexahydro-2H-pyrimido[1,2-a]pyrimidine) has been reported, alongside subsequent coordination chemistry;^[25,26] and there is an early report of sigma complexes formed from cyclic diboranes.^[27] Shore and co-workers have developed the coordination chemistry and reactivity of related cyclic anionic organohydroborates of the early transition metals.^[28]

In this contribution we report the coordination chemistry of various N-substituted cyclic 1,2-BN-cyclohexanes, using {Ir(PCy₃)₂(H)₂}⁺ or {Rh(chelating-diphosphine)}⁺ fragments, to afford the resulting sigma-complexes. We also comment on their subsequent dehydrogenation/dehydrocoupling that leads to insight into both: 1) the active species involved, and 2) the metal-free cyclic amine-borane intermediates formed during these transition-metal-catalysed routes, which operate at a significantly lower temperature than non-catalysed or heterogeneously catalysed alternatives.

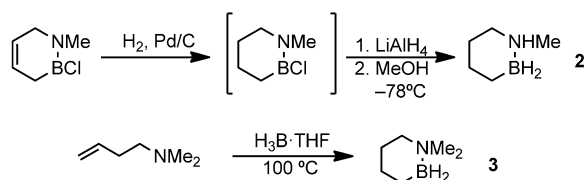
Results and Discussion

Synthesis of cyclic amine-boranes

To provide a comparison of the effect of increasing substitution at nitrogen with regard to both coordination chemistry and subsequent dehydrogenation, three 1,2-BN-cyclohexanes were prepared (Scheme 1A): 2,2-H₂-1,2-B,N-C₄H₁₀ (**1**), 2,2-H,Me-1,2-B,N-C₄H₁₀ (**2**) and 2,2-Me₂-1,2-B,N-C₄H₁₀ (**3**). The synthesis of compound **1** has recently been reported by hydroboration of a bistrimethylsilyl-substituted homoallylamine by one of us.^[9] Compound **2** is, to our knowledge, unreported in the open literature as an isolated compound^[29] while compound **3** was originally reported by Wille and Goubeau in 1972.^[30] We have isolated compounds **2** and **3** (see Experimental Section) as an analytically pure powder or liquid, respectively (Scheme 3). The ¹¹B and ¹H B-H NMR chemical shifts for these three compounds are also given for later comparison with their coordination complexes.

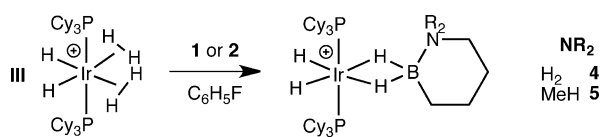
Reactivity with [Ir(PCy₃)₂(H)₂(H)₂][BAR^F₄]

Addition of one equivalent of cyclic amine-borane **1** to a C₆H₅F solution of in situ generated [Ir(PCy₃)₂(H)₂(H)₂][BAR^F₄], **III** (a source of the {Ir(PCy₃)₂(H)₂}⁺ fragment),^[16,17] resulted in the formation of the complex [Ir(PCy₃)₂(H)₂(η²-H₂BNH₂C₄H₈)] [BAR^F₄] (**4**)^[31] in quantitative yield as measured by ¹H, ¹¹B and ³¹P NMR spectroscopies (Ar^F₄ = 3,5-(CF₃)₂C₆H₃, Scheme 4). Complex **4** can be characterised as a Shimoi-type sigma-amine-borane complex.^[14,15,32] Analytically pure, crystalline, material was isolated



	NR ₂	$\delta(^{11}\text{B})$	$\delta(^1\text{H}) \text{BH}_2$
1	HH	-11.3 [95 Hz]	1.81
2	MeH	-6.5 [96 Hz]	2.05
3	Me ₂	-3.0 [97 Hz]	2.54

Scheme 3. Synthesis of the 1,2-BN-cyclohexanes and key NMR spectroscopic data [$J(\text{BH})$ in parenthesis in CD_2Cl_2].



Scheme 4. Synthesis of cyclic amine borane complexes of the $\{\text{Ir}(\text{PCy}_3)_2(\text{H})_2\}^+$ fragment. $[\text{BAR}_4]^-$ anions are not shown.

by recrystallisation at low temperature from $\text{C}_6\text{H}_5\text{F}$ /pentane solution.

The solid-state structure of complex **4** is shown in Figure 1, and confirms the formulation. The Ir–H were located in the final difference map, while the bridging B–H–Ir were not located with any reliability and placed in calculated positions. The Ir...B [2.217(4) Å], B1–C1 [1.588(6) Å] and B1–N1 [1.605(6) Å] distances are all consistent with an amine-borane taking part in two Ir...H–B 3 center-2 electron interactions, comparing closely with sigma complexes of $\text{H}_3\text{B}\cdot\text{NMe}_3$ [Ir...B, 2.207(7) Å],^[17] $\text{H}_3\text{B}\cdot\text{NMeH}_2$ [2.210(7) Å]^[33] and $\text{H}_3\text{B}\cdot\text{NH}_3$ [2.209(5) Å]^[18] with the same metal fragment. Amine-boranes acting in a monodentate bonding mode through a single B–H bond, or as B–H activated boryls, show significantly longer (ca. 2.6 Å or longer)^[34,35] and shorter M–B distances (less than 2.1 Å), respectively.^[36,37] The cyclic amine-borane adopts a chair conformation (Figure 1B), meaning there is no plane of symmetry in the molecule in the solid state.

In solution (CD_2Cl_2), the ^{11}B NMR spectrum of **4** shows a diagnostic,^[38,39] and significant, downfield shift on coordination with the metal, $\delta = 19.8$ ppm, when compared to free ligand, $\delta = -11.3$ ppm. This signal is broad (fwhm = 350 Hz) masking the expected reduction in $J(\text{BH})$.^[15] The ^1H NMR spectrum displays a single Ir–H environment at $\delta = -20.53$ ppm [t, $J(\text{PH}) = 16$ Hz] and a single Ir–H–B environment at $\delta = -6.23$ ppm (br) that sharpens on decoupling of ^{11}B and is shifted 8.04 ppm upfield from **1**. Finally, the ^1H NMR spectrum shows a single N–H environment at $\delta = 4.07$ ppm (confirmed by $^1\text{H}/^1\text{H}$ COSY and HSQC experiments). The $^{31}\text{P}\{^1\text{H}\}$ NMR spectrum displays two environments that show mutual ^{31}P – ^{31}P coupling, consistent with a *trans* orientation: $J(\text{PP}) = 268$ Hz. These solution data are consistent with a sigma-amine-borane complex, interacting

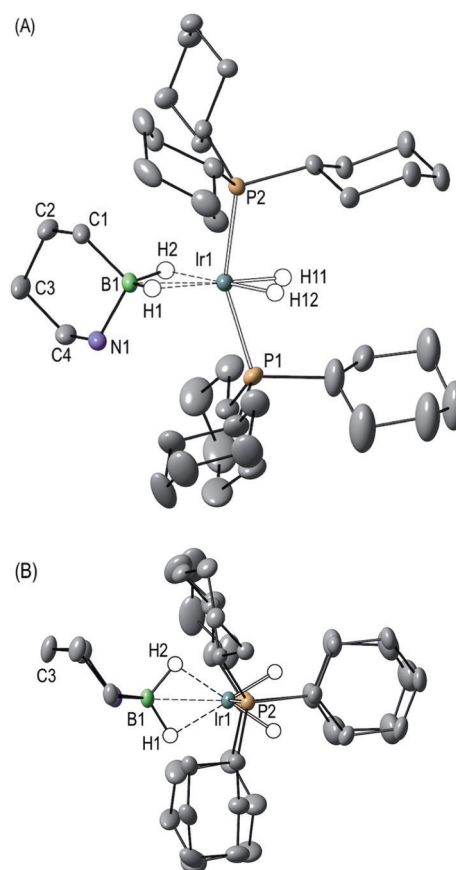


Figure 1. Solid-state structure of the cationic portion of complex **4**, side (A) and plan (B) view. Displacement ellipsoids are shown at the 30% probability level. Selected bond lengths [Å] and angles [°]: Ir1–B1, 2.217(4); Ir1–P1, 2.3145(11); Ir1–P2, 2.3244(10); B1–C1, 1.588(6); B1–N1, 1.605(6); P1–Ir1–P2, 155.87(4).

through two B–H...Ir interactions, in which the cyclic amine-borane is undergoing a fluxional process that gives a time-averaged mirror plane that makes the two sets of hydride ligands equivalent. A simple ring-flip is suggested, rather than a rotation around the B1–Ir1 vector that would also make the phosphine ligands equivalent,^[40] and for the free amine-borane this ring-flip has been shown to proceed through a low barrier ($8.8(\pm 0.2)$ kcal mol⁻¹).^[9]

The corresponding sigma complex of **2**, $[\text{Ir}(\text{PCy}_3)_2(\text{H})_2(\eta^2\eta^2\text{-H}_2\text{BNHMeC}_4\text{H}_8)][\text{BAR}_4]$ (**5**), can be prepared in a manner similar to **4**. The synthesis of **5** by displacement of the dihydrogen ligand in **III** takes longer than for **4**: 90 min compared to on time of mixing, respectively. The solid-state structure of complex **5** is shown in Figure 2, which shows it to be very similar to that of **4**, with the amine-borane also adopting a chair conformation. Unlike **4**, the BN-cyclohexane ligand is disordered, occupying four chemically identical, but crystallographically different sites (see the Supporting Information). The Ir...B distance measured using this model, 2.230(4) Å, is within error the same as for **4**, as is the P1–Ir–P2 angle of 155.13(3)°.

Despite repeated attempts, only a few crystals of complex **5** were produced, with the complex forming as an oil on attempts to re-crystallise, meaning that analytically pure material

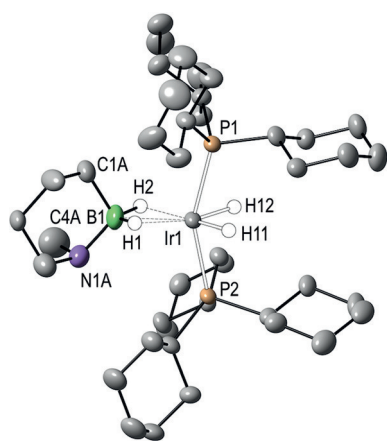


Figure 2. Solid-state structure of the cationic portion of complex **5**. Only one disordered component of the cyclic amine-borane ligand is shown. Displacement ellipsoids are shown at the 30% probability level. Selected bond lengths [Å] and angles [°]: Ir1-B1, 2.230(4); Ir1-P1, 2.3269(7); Ir1-P2, 2.3266(7); B1-C1, 1.588(5); B1-N1, 1.566(6); P1-Ir1-P2, 155.13(3).

for microanalysis was not available. Nevertheless, NMR spectroscopy demonstrates the formulation of **5** in the bulk. In the ^1H NMR spectrum the Ir–H groups are now observed as two relative 1-H signals, at $\delta = -20.58$ and -20.82 ppm, due to the asymmetry now imposed by the NMe group on the cyclic amine-borane that would not be removed by a low energy ring-flip. Likewise, two Ir–H–B signals are observed ($\delta = -6.24$, -6.35 ppm), and a more complicated aliphatic region compared with **4** is noted, as all the methylene C–H groups are now inequivalent. The ^{11}B NMR spectrum shows a signal at $\delta = 22.4$ ppm, similar to that measured for complex **4** and shifted downfield from free ligand ($\delta = -6.5$ ppm). As with **4**, there are two environments observed in the $^{31}\text{P}\{^1\text{H}\}$ NMR spectrum that show *trans* $J(\text{PP})$ -coupling [$J(\text{PP}) = 276$ Hz].

Addition of **3** to a $\text{C}_6\text{H}_5\text{F}$ solution of $[\text{Ir}(\text{PCy}_3)_2(\text{H}_2)_2(\text{H})_2][\text{BAR}^{\text{F}}_4]$ resulted in no reaction to the detection limit of $^{31}\text{P}\{^1\text{H}\}$ NMR spectroscopy (ca. 5%) in a sealed NMR tube. However, the ^1H NMR spectrum showed a very small peak at $\delta = -4.06$ ppm (less than 5%) that might be assigned to a sigma complex by comparison with the well-characterized examples **4** and **5**. This might suggest an initial equilibrium is established between the starting bis-dihydrogen complex and a corresponding BN-cyclohexane sigma-complex that favours the starting material (presumably due to the steric clash between the PCy_3 and the NMe_2 groups). With the same metal fragment we have previously commented upon similar relative differences in the strength of the Ir–H–B sigma interaction when comparing $\text{H}_3\text{B}\cdot\text{NR}_3$ ($\text{R} = \text{H}$ or Me).^[17,18] Over time (8 h), decomposition to $[\text{Ir}(\text{PCy}_3)_2\text{H}_5]$ ^[41] and $[\text{Ir}_2\{(\text{PCy}_3)_2\}_2\text{H}_5][\text{BAR}^{\text{F}}_4]$ ^[17] is observed.

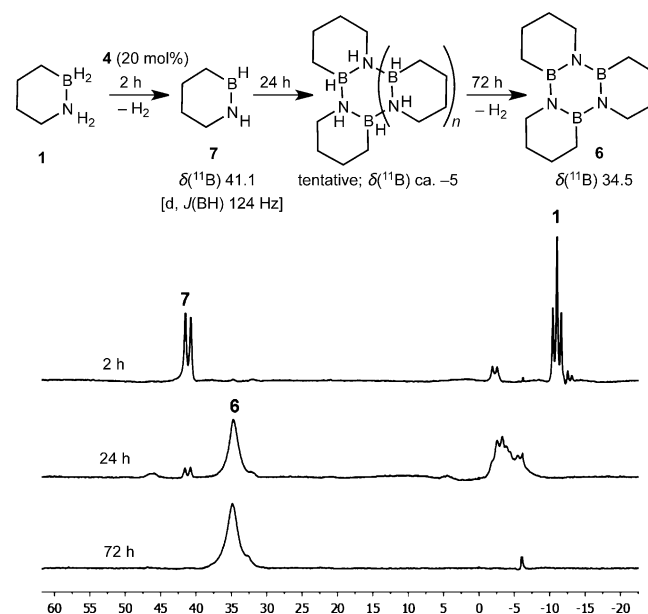
Catalytic dehydrocoupling using the Ir–BN complexes

When prepared pure, complexes **4** and **5** are stable for at least 24 h in $1,2\text{-F}_2\text{C}_6\text{H}_4$ solution with no significant change observed by NMR spectroscopy. However, addition of five additional equivalents of the cyclic amine-borane **1** to complex **4** (i.e.,

20 mol%) results in the slow (72 h, $\text{TOF} \approx 0.07 \text{ h}^{-1}$, sealed NMR tube) dehydrocoupling to form the final amino-borane derived tricyclic borazine product $[\text{BNC}_4\text{H}_8]_3$ **6** [$\delta = 34.5$ ppm, s; lit. 34.8, C_6D_6],^[9,30] (Scheme 5). Inspection of the ^{11}B NMR spectrum after 2 h shows compound **1** and a significant proportion of a new signal assigned to the new monomeric amino-borane HBNHC_4H_8 , **7** [$\delta = 41.1$ ppm, d, $J(\text{BH})$ 124 Hz]. This chemical shift and coupling pattern is similar to other, transient, amino-boranes,^[17,42,43] as well as stable $\text{HBNMeC}_4\text{H}_8$ **8** (vide infra). After 24 h the signal due to **7** had essentially disappeared, with **6** now observed as a significant product. Also apparent after 24 h is a set of broad peaks centred around $\delta = -5$ ppm that also show $J(\text{BH})$ coupling. Over a further 48 h (72 h in total) these signals reduce in intensity at the overall gain of **6**, and the temporal behaviour of the system suggests they are due to intermediates that follow **7** and precede **6**. The final organometallic product observed is the pentahydride $[\text{Ir}(\text{PCy}_3)_2\text{H}_5]$.^[41] Reformation of compound **1** was not observed during these later processes; the observation of which would point to H-redistribution processes.^[42,44]

Due to their transient nature, overlapping signals, and lack of charge, we have not been able to use detailed NMR spectroscopic or ESI-MS techniques to determine the identity of these intermediate species. The chemical shift/coupling constant data suggest four-coordinate BH groups that are not metal-bound, possibly due to a cycloborazane species (dimers and/or trimers, e.g., $n = 0$ or 1 , Scheme 5) and isomers thereof.

In order to put the structures of these intermediates on a firmer footing we have used DFT geometry optimization coupled with GIAO ^{11}B chemical shift calculations to help in their identification. Table 1 shows selected examples, with full details given in the Supporting Information. The chemical shifts of compounds **7** [exptl $\delta = 41.1$ ppm, calcd $\delta = 38.4$ ppm] and **6** [exptl $\delta = 34.5$ ppm, calcd $\delta = 31.9$ ppm] are reproduced well,

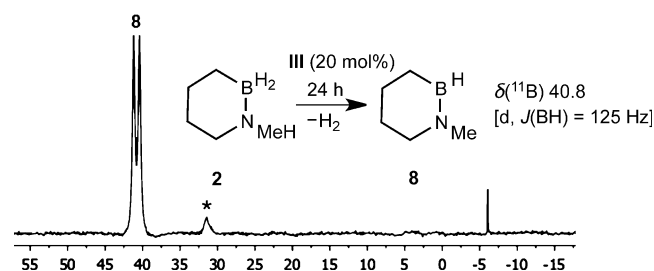


Scheme 5. Dehydrocoupling of **1** catalysed by **4**. ^{11}B NMR spectrum (ppm scale) at 2, 24 and 72 h.

with a consistent small, approximately 2.5 ppm, difference between experiment and calculation (Table 1). Based on these calculations diborazane and triborazane species would be expected to show signals between $\delta = 0$ to -7 ppm and $\delta = -2$ to -9 ppm, respectively, in the experimentally determined spectrum as is observed (Scheme 5). Partially dehydrogenated trimers would be expected to show an additional signal about $\delta = +37$ ppm, very similar to **6**, and thus might be obscured. The oligomerisation of amino-boranes to form cyclic borazane products is well-known, and these can, in certain cases, be further dehydrogenated by a transition metal-catalyst to form cyclic borazines.^[22,45,46]

Addition of 5 equivalents of **2** to a 1,2-F₂C₆H₄ solution of **III** (as a precursor to **5**) in a sealed NMR tube results in dehydrogenation and the formation of the monomeric cyclic amino-borane HBNMeC₄H₈ **8** (Scheme 6) after 24 h (TOF ≈ 0.2 h⁻¹). Compound **8** was initially reported by Wille and Goubeau,^[30] and has been independently prepared by intramolecular hydroboration of the *N*-methylhomoallylamine-borane adduct and subsequent one-pot thermal dehydrogenation (see Experimental Section). Compound **8** does not cyclotrimerise or cyclodimerise and remains monomeric in solution, as evidenced by a characteristic down-field chemical shift in the ¹¹B NMR spectrum $\delta = 40.8$ ppm [$J(\text{BH})$ 125 Hz], very similar to **7**. No other significant boron-containing products were observed during this process. The final organometallic species observed were **5** and Ir(PCy₃)₂H₅ as identified by ¹H and ³¹P{¹H} NMR spectroscopy, in a 0.6:1 ratio, respectively.

The {Ir(PCy₃)₂(H)₂}⁺ fragment thus acts as a slow catalyst (or precatalyst) for the dehydrogenation of these cyclic amine-boranes, as found for their acyclic counterparts.^[17,18,42] That the onward dehydrogenation does not occur in **4** or **5** in the absence of additional amine-borane is a further demonstration of the promotional role that amine-borane plays in dehydrogenation chemistry. This is likely through the formation of B–H...H–N dihydrogen bonds,^[47,48] which are commonplace in amine-borane chemistry, and have been shown by computational



Scheme 6. Dehydrogenation of **2** catalysed by **5**. ¹¹B NMR spectrum after 24 h (ppm scale). *: Assigned to trace 1-OH-2-Me-1,2-B,N-C₄H₈^[30] (confirmed by EI-MS). The signal at $\delta = -6.1$ ppm is assigned to residual [BArF₄]⁻.

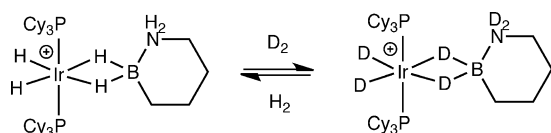
techniques to play an important role in lowering the barrier to B–H and N–H activation steps.^[18,49–51] We have not explored the mechanism for the dehydrogenation process in **4** and **5** in detail, but other studies using this iridium fragment have shown that N–H activation of amine-boranes is rate-determining and preceded by B–H activation.^[18,49]

Interestingly, in this context, addition of D₂ to complex **4** in C₆H₅F solution results in the loss of the Ir–H, Ir–H–B and N–H resonances in the ¹H NMR spectrum, and the appearance of corresponding signals in the ²H NMR spectrum while the ³¹P{¹H} NMR spectrum remains unchanged (Scheme 7). Dissolved HD and H₂ were also observed [$\delta = 4.47$ ppm, t, $J(\text{HD}) = 43$ Hz; $\delta = 4.50$ ppm, respectively]. This points to both rapid Ir–H/D₂ exchange,^[40] and that sequential N–H or B–H activation (in either order) are of approximately similar energies and reversible. An alternative mechanism would be a concerted and reversible NH and BH activation that leads to amino-borane, **7** that then re-adds D₂. That no free amino-borane **7**, or the final cyclic trimer **6**, were observed argues against a mechanism involving such reversible dehydrogenation.^[52]

Addition of D₂ followed by H₂ re-establishes the N–H ($\delta = 4.07$ ppm), Ir...H–B ($\delta = -6.23$ ppm) and Ir–H ($\delta = -20.53$ ppm) signals, showing that this process is reversible. N–H activation

Table 1. Calculated ¹¹B NMR chemical shifts of representative dimers and trimers (σ = standard (BF₃·OEt₂) - molecule).

Molecule	σ (ppm)	Molecule	σ (ppm)
	+38.4 [exptl +41.1]		+31.9 [exptl 34.5]
	-9.3		-2.2
	-10.7 (B1) +34.3 (B2) -9.1 (B3)		-11.0 (B1) -9.3 (B2) -5.6 (B3)



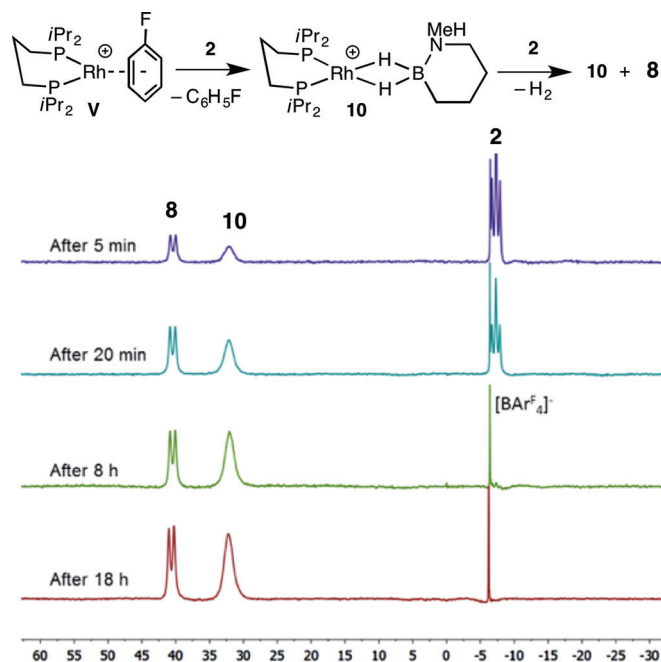
Scheme 7. Reversible H/D exchange in complex **4**. $[\text{BAR}^{\text{F}}_4]^-$ anions are not shown.

is generally considered to have a larger barrier than B–H activation in cationic systems.^[1,17,53,54] For example, addition of D_2 to $[\text{Ir}(\text{PCy}_3)_2(\text{H})_2(\eta^2\eta^2\text{-H}_3\text{BNMeH}_2)][\text{BAR}^{\text{F}}_4]$ results in H/D exchange only at Ir–H and B–H.^[33] However, products that arise from formal N–H activation over B–H activation have been isolated^[55,56] or postulated^[57,58] for neutral systems and are also proposed as intermediates in amine-borane dehydrogenation.^[20,59] It thus appears likely that the cyclic nature of the amine-borane in **5** results in more levelled B–H/N–H activation energies. N–H activation may be additionally assisted by intramolecular hydrogen bonding.^[57,60] Related acyclic phosphido-borane complexes have been isolated and shown to undergo rapid and reversible P–H/B–H bond activation as probed by H/D scrambling experiments.^[61] As significant D incorporation into the PCy_3 ligand is also observed, we cannot discount more complicated mechanisms for H/D exchange that involve cyclometallated phosphine ligands.

Reactivity of cyclic amine–boranes with $[\text{Rh}(i\text{Pr}_2\text{PCH}_2\text{CH}_2\text{CH}_2\text{P}i\text{Pr}_2)(\eta^6\text{-C}_6\text{H}_5\text{F})][\text{BAR}^{\text{F}}_4]$

Addition of **2** equivalents of the cyclic amine-borane **2** to $[\text{Rh}(i\text{Pr}_2\text{PCH}_2\text{CH}_2\text{CH}_2\text{P}i\text{Pr}_2)(\eta^6\text{-C}_6\text{H}_5\text{F})][\text{BAR}^{\text{F}}_4]$, **V**,^[62] in 1,2- $\text{F}_2\text{C}_6\text{H}_4$ solution and monitoring in situ using $^{31}\text{P}\{^1\text{H}\}$ and ^{11}B NMR spectroscopy showed that after 5 min a new complex was formed $[\text{Rh}(i\text{Pr}_2\text{PCH}_2\text{CH}_2\text{CH}_2\text{P}i\text{Pr}_2)(\eta^2\eta^2\text{-H}_2\text{BNHMeC}_4\text{H}_8)][\text{BAR}^{\text{F}}_4]$ (**10**; Scheme 8), alongside unreacted **V** and **2**. Also observed is the amino-borane **8**. Over time **V** and **2** are consumed, so that after 8 h **10** and **8** remain. Over this time period a small amount of dimer $[\text{Rh}_2(i\text{Pr}_2\text{PCH}_2\text{CH}_2\text{CH}_2\text{P}i\text{Pr}_2)_2\text{H}_5][\text{BAR}^{\text{F}}_4]$ (**12**) also forms ($\approx 5\%$ by $^{31}\text{P}\{^1\text{H}\}$ and ^1H NMR spectroscopy), vide infra. Complex **10** can be produced as a red, analytically pure, crystalline material in moderate (40–45%) yield by recrystallization of the reaction mixture from 1,2- $\text{F}_2\text{C}_6\text{H}_4$ /pentane at -35°C . When isolated pure, **10** is relatively stable, as is the case with the iridium complexes. After 2 days, isolated samples of **10** in $\text{C}_6\text{H}_5\text{F}$ solution decompose to give only **V** and an unidentified borane species [$\delta(^{11}\text{B}) = 5.17$ ppm (s)]. The observation of both the starting material, **V**, and amino-borane, **8**, under conditions of excess **2** suggests that initial substitution of the fluorobenzene ligand is slower than subsequent amine-borane promoted dehydrogenation in **10** (Scheme 8).

The room temperature ^1H NMR spectrum of **10** shows a set of broadened environments for the chelating ligand and amine-borane that give little further information. Two high-field signals at $\delta = -4.9$ ppm and $\delta = -5.4$ ppm are assigned to the Rh–H–B groups. Although two signals are observed, showing that the amine-borane lacks a plane of symmetry due to the NMe group, only one signal is observed in the $^{31}\text{P}\{^1\text{H}\}$



Scheme 8. ^{11}B NMR spectra (ppm scale) showing the temporal evolution of the dehydrogenation of **2** (2 equivalents) by **V** to form $[\text{Rh}(i\text{Pr}_2\text{PCH}_2\text{CH}_2\text{CH}_2\text{P}i\text{Pr}_2)(\eta^2\eta^2\text{-H}_2\text{BNHMeC}_4\text{H}_8)][\text{BAR}^{\text{F}}_4]$ (**10**) and amino-borane **8**. $[\text{BAR}^{\text{F}}_4]^-$ anions are not shown.

NMR spectrum at room temperature [$\delta = 57.9$ ppm, $J(\text{RhP}) = 162$ Hz]. Cooling to 190 K reveals two signals [$\delta = 57.8$ ppm, dd, $J(\text{PP}) = 56$ Hz, $J(\text{RhP}) = 160$ Hz; $\delta = 56.9$ ppm, dd, $J(\text{PP}) = 56$ Hz, $J(\text{RhP}) = 160$ Hz]. This suggests a fluxional process that makes equivalent the two phosphine groups. A mechanism that invokes a bidentate to monodentate change in amine-borane binding and then a rotation around the remaining Rh–H bond is suggested.^[40] The ^{11}B NMR spectrum shows a broad signal at $\delta = 32.1$ ppm, downfield shifted from free **2** by 38.6 ppm, consistent with a bidentate binding mode of the amine-borane at a Rh^{I} centre.^[21]

Figure 3 shows the solid-state structure of the cationic portion of complex **10**, demonstrating that the cyclic amine-borane, **2**, interacts with the Rh centre in a bidentate manner through two Rh–H–B interactions at a pseudo-square planar Rh^{I} centre. Although the bridging hydrogen atoms were located in the final difference map they were ultimately placed in calculated positions. The amine-borane is equally disordered over two positions, which can be modelled as either the NMe pointing axial or equatorial with respect to the RhP_2 plane. The Rh...B distance measured from this model at 2.150(6) Å is slightly shorter, but still similar, to that in closely related $[\text{Rh}(\text{Ph}_2\text{PCH}_2\text{CH}_2\text{CH}_2\text{PPh}_2)(\eta^2\eta^2\text{-H}_3\text{B-NMe}_3)][\text{BAR}^{\text{F}}_4]$, 2.199(3) Å.^[19] The cyclic amine-borane adopts a chair conformation in **10**.

Addition of 2 equivalents of **1** to **V** results, after only 30 min, in the formation of the new complex $[\text{Rh}(i\text{Pr}_2\text{PCH}_2\text{CH}_2\text{CH}_2\text{P}i\text{Pr}_2)(\eta^2\eta^2\text{-H}_2\text{BNH}_2\text{C}_4\text{H}_8)][\text{BAR}^{\text{F}}_4]$ (**9**) and the complete consumption of the amine-borane to form the amino-borane **7** (Scheme S2, Supporting Information). Over 8 h, this mixture evolves by further dehydrocoupling to give cyclotriborazine **6** and complex **9** as the organometallic product. At the early

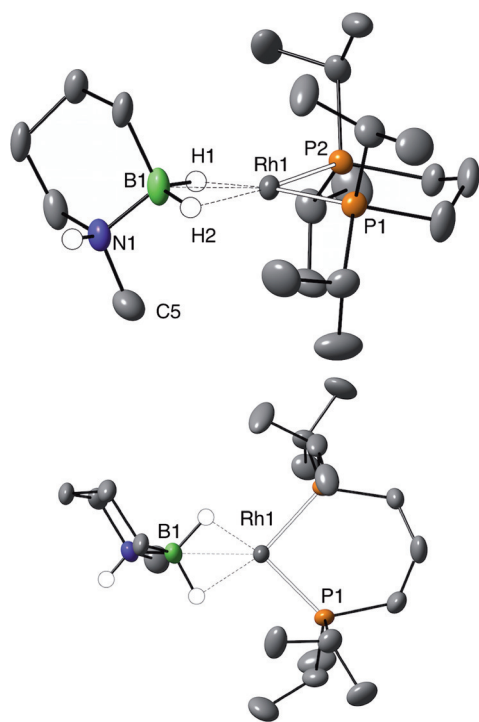


Figure 3. Solid-state structure of the cationic portion of complex **10** (side and top view). Only hydrogen atoms associated with the NH and Rh...HB interaction are shown, and only one disordered component is shown. Displacement ellipsoids are shown at the 30% probability level. Selected bond lengths [Å] and angles [°]: Rh1-B1, 2.150(6); Rh1-P1, 2.2167(12); Rh1-P2, 2.2030(12); B1-N1, 1.518(8); P1-Rh1-P2, 92.95(5).

stages of the reaction, NMR signals due to amine-borane and the sigma-complex **9** are too broad to be observed in the ^1H and ^{11}B NMR spectra, but the $^{31}\text{P}\{^1\text{H}\}$ NMR spectrum is sharper, thus suggesting a rapid exchange between bound and free amine-borane. In support of this rapid exchange hypothesis, when all of **1** is consumed, and the opportunity for exchange is reduced, sigma-complex **9** is observed as a characteristic broad signal at $\delta=29.3$ ppm in the ^{11}B NMR spectrum while the Rh-H-B groups are observed at $\delta=-4.83$ ppm in the ^1H NMR spectrum as a broad signal (relative integral of 2H). The $^{31}\text{P}\{^1\text{H}\}$ NMR spectrum shows a single environment that couples to ^{103}Rh [$\delta=57.1$ ppm, $J(\text{RhP})=160$ Hz]. As this rapid exchange is not observed in **10** or **11**, we suggest that the increasing levels of substitution on nitrogen slow down this process, which might indicate an associative mechanism for ligand substitution. Recrystallisation of the reaction mixture from 1,2- $\text{F}_2\text{C}_6\text{H}_4$ /pentane resulted in a small number of red crystals of complex **9** that required mechanical separation from co-crystallised orange **V**. The solid-state structure of complex **9** is shown in Figure 4, and is closely related to **10**. In particular, the Rh...B and B-N distances are the same within error or very similar, respectively: 2.155(5) and 1.588(6) Å. As complex **9** cannot be isolated pure in bulk, we have not pursued the H/D exchange experiments.

Addition of cyclic-amine-borane **3** to **V** in 1,2- $\text{F}_2\text{C}_6\text{H}_4$ solution results in the slow (24 h) substitution of the arene and the formation of $[\text{Rh}(\text{iPr}_2\text{PCH}_2\text{CH}_2\text{CH}_2\text{P}(\text{iPr}_2)(\eta^2\text{-}\eta^2\text{-H}_2\text{BNMe}_2\text{C}_4\text{H}_8))][\text{BAR}^{\text{F}}_4]$

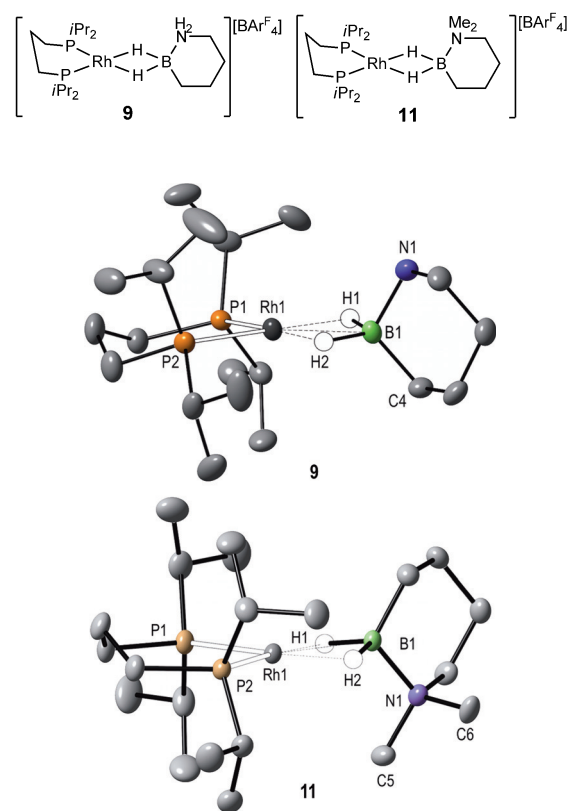


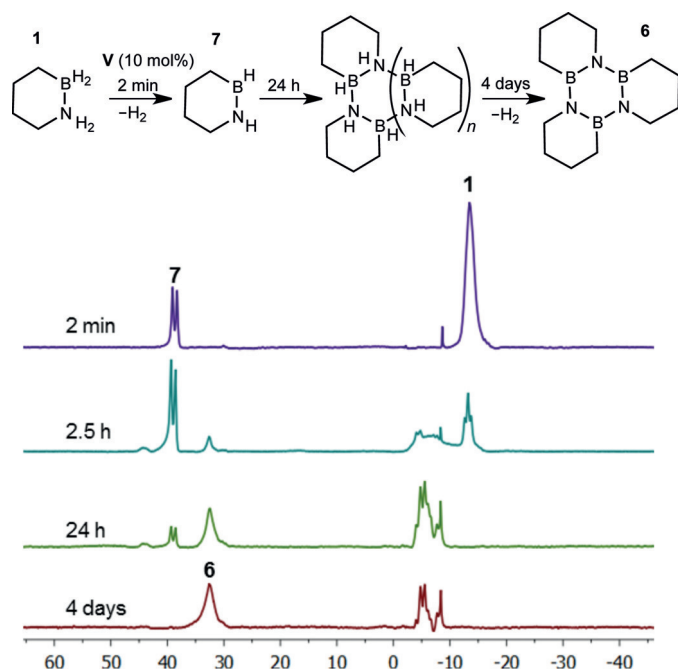
Figure 4. Solid-state structures of the cationic portion of complexes **9** and **11**. Only hydrogen atoms associated with the Rh...HB interaction are shown. Displacement ellipsoids are shown at the 30% probability level. Selected bond lengths (Å) and angles (°) (**9**): Rh1-B1, 2.155(5); Rh1-P1, 2.2174(12); Rh1-P2, 2.2170(12); B1-N1, 1.588(6); P1-Rh1-P2, 93.52(5). (**11**) Rh1-B1, 2.172(3); Rh1-P1, 2.2204(8); Rh1-P2, 2.2182(8); B1-N, 1.599(4); P1-Rh1-P2, 94.14(3).

(**11**) which can be recrystallised by addition of pentane. Complex **11** has been characterized by NMR spectroscopy and single-crystal X-ray diffraction, and shows very similar data to that of **9** and **10**. The ^1H NMR spectrum shows a single NMe_2 environment at $\delta=2.85$ ppm (6H) and a single Rh-H-B environment at $\delta=-5.17$ ppm, while the ^{11}B NMR spectrum shows a down-field shifted signal at $\delta=34.4$ ppm. The solid-state structure (Figure 4) also reflects these similarities with the pseudo-square planar Rh^{I} centre coordinated with the cyclic amine-borane in a bidentate manner. Comparing **9**, **10**, and **11**, there is no change in the Rh...B bond distances [2.155(5), 2.150(6), 2.172(3) Å, respectively] within the experimental error. There is a slight change in chemical shift of the boron atom when compared with free ligand [$\Delta\delta=+40.6$, $+38.6$, $+37.4$ ppm], which suggests a trend in that increasing N-substitution leads to a decreasing M...B interaction that is not captured by an associated change in bond lengths.^[38,63]

Catalytic dehydrogenation using the Rh-BN complexes

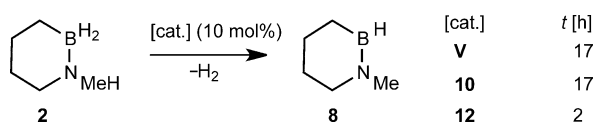
We have explored the catalytic dehydrogenation/dehydrocoupling of the cyclic amine-boranes **1** and **2** using the $\{\text{Rh}(\text{iPr}_2\text{PCH}_2\text{CH}_2\text{CH}_2\text{P}(\text{iPr}_2))\}^+$ fragment. Using 10 mol% **V** slow

(4 days, sealed system, TOF $\approx 0.1 \text{ h}^{-1}$) dehydrocoupling of **1** occurs to ultimately afford the tricyclicborazine **6**. As with catalyst **4**, intermediate species centred around $\delta = -5 \text{ ppm}$ are observed in the ^{11}B NMR spectrum (Scheme 9, Table 1). At the end of catalysis complexes **9** and dimeric **12** $[\text{Rh}_2(\text{iPr}_2\text{PCH}_2\text{CH}_2\text{CH}_2\text{P}(\text{iPr})_2)_2\text{H}_3][\text{BAR}^{\text{F}}_4]$ are observed as the organometallic species.



Scheme 9. ^{11}B NMR spectra (ppm scale) showing the temporal evolution of the dehydrogenation of **1** by **V** (10 mol%) to ultimately form **6**.

Dehydrogenation of methyl-substituted amine-borane **2** using **V** (10 mol%) results in the formation of amino-borane **8**, taking 17 h (TOF $\approx 0.6 \text{ h}^{-1}$; Scheme 10) in a sealed NMR tube. Following the catalyst speciation by $^{31}\text{P}\{^1\text{H}\}$ NMR spectroscopy showed that **V** was replaced by **10** and then **12**, the ratio of which changed over time, to finally give a ratio of **10**:**12** of 1:9 after 17 h.



Scheme 10. Dehydrocoupling of **2** using catalyst **V** to afford amino-borane **8**.

The formation of the dimer $[\text{Rh}_2(\text{iPr}_2\text{PCH}_2\text{CH}_2\text{CH}_2\text{P}(\text{iPr})_2)_2\text{H}_3][\text{BAR}^{\text{F}}_4]$ (**12**) is interesting, and to explore its role further it was synthesized independently by addition of $[\text{H}(\text{OEt}_2)_2][\text{BAR}^{\text{F}}_4]$ ^[64] to Fryzuk's dinuclear $[\text{Rh}(\text{iPr}_2\text{PCH}_2\text{CH}_2\text{CH}_2\text{P}(\text{iPr})_2)(\mu\text{-H})_2]$ complex^[65] under an atmosphere of H_2 . Complex **12** can be isolated in good yield as a microcrystalline material and has been characterized by ^1H , ^{31}P NMR spectroscopy and microanalysis

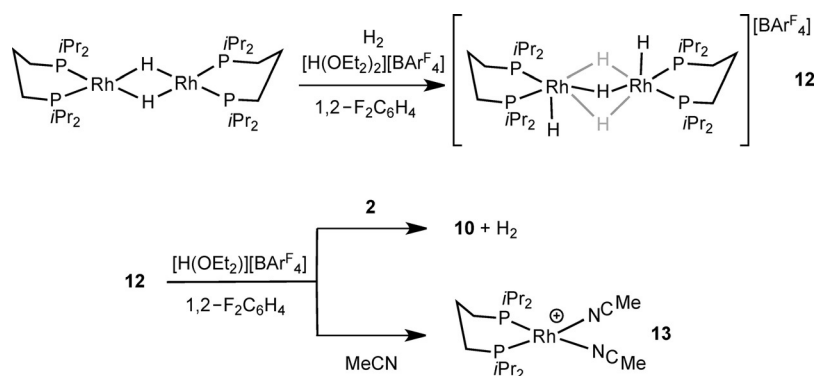
(Scheme 11). A single crystal X-ray diffraction study demonstrated the gross structure, but the hydrides were not located (see Supporting Information). Complex **12** is similar to previously reported $[\text{Rh}_2(\text{bis-phosphine})_2\text{H}_3]^+$ cations that are formed by hydrogenation of $[\text{Rh}(\text{bis-phosphine})]^+$ precursors, through dimerisation/deprotonation.^[66–68] It is stable to H_2 loss under vacuum (10^{-3} Torr) in the solid-state and in solution. We did not observe any evidence for the formation of boronium cations (e.g., $[\text{L-BHNHMe}(\text{CH}_2)_4]^+$) which might indicate a hydride abstraction route to form intermediate monocationic systems with odd numbers of hydrides.^[69]

Complex **12** is a competent catalyst itself for the dehydrogenation of compound **2**, taking approximately 2 h to effect complete conversion ($[\text{Rh}] = 10 \text{ mol\%}$, sealed NMR tube, TOF = 5 h^{-1}). When comparing **10** and **12** as catalysts (10 mol% $[\text{Rh}]$) both follow an overall first-order profile ($k = 1.18(3) \times 10^{-5} \text{ s}^{-1}$; $2.16(7) \times 10^{-4} \text{ s}^{-1}$, respectively) with dimeric **12** much faster than monomeric **10**. No induction period was observed.^[19,20] As these are sealed conditions, inhibition by H_2 may well be occurring, complicating a detailed kinetic analysis, as observed previously for Rh systems.^[20,70] Unfortunately, we have been unable to reliably measure the rate in an open system (under Ar) due to partial decomposition of **8** upon sampling.^[30]

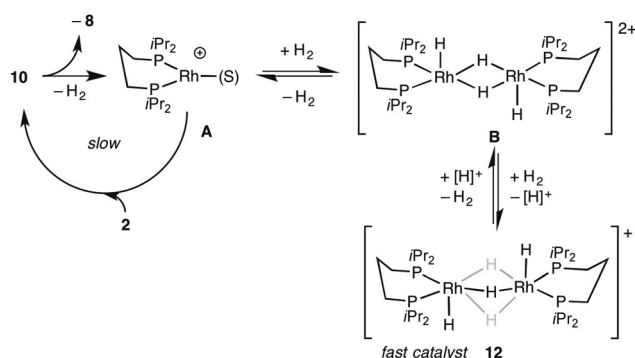
Addition of a hindered base (2,6-di-*tert*-butylpyridine, 5 equivalents relative to catalyst) to the mixture with **10/2** resulted in faster catalysis ($k = 1.4(1) \times 10^{-4} \text{ s}^{-1}$) and the observation of **12** as the only organometallic species at the end of catalysis. Addition of $[\text{H}(\text{OEt}_2)_2][\text{BAR}^{\text{F}}_4]/10$ equivalents of **2** to dimer **12** resulted in the formation of **10** and catalysis at a slower rate, similar to starting from **10** ($k = 2.3(1) \times 10^{-5} \text{ s}^{-1}$). Addition of $[\text{H}(\text{OEt}_2)_2][\text{BAR}^{\text{F}}_4]/\text{CH}_3\text{CN}$ to dimer **12** resulted in the formation of $[\text{Rh}(\text{iPr}_2\text{PCH}_2\text{CH}_2\text{CH}_2\text{P}(\text{iPr})_2)(\text{NCMe})_2][\text{BAR}^{\text{F}}_4]$ (**13**; Scheme 11). Complex **13** was also independently synthesized by the addition of CH_3CN to **V**. These, and our previous observations, suggest: 1) dimeric **12** is a more active (pre)catalyst than monomeric **10**; 2) under catalytic conditions, **12** forms from **10** by slow dehydrogenation of **2**, subsequent oxidative addition of H_2 and dimerization to form intermediate **B**, which adds further H_2 and is reversibly deprotonated to form $[\text{H}(\text{solvent})_x][\text{BAR}^{\text{F}}_4]$ and **12** (Scheme 12); 3) H^+ inhibits catalysis presumably by channelling the resting state away from **12**; 4) addition of base promotes the formation of **12**.

That dimeric **12** is an active catalyst or precatalyst for amine-borane dehydrogenation has resonance with previous reports of dimeric $\{\text{Rh}(\text{L}_2)\}_2$ being implicated in dehydrocoupling of acyclic amine-boranes,^[19,58,70,71] although in some systems dimers have been discounted on the basis of computational analysis.^[49] The likely involvement of potential dimer/monomer equilibria during catalysis using **12** as a precursor was probed using the method of initial rates, monitoring over the first 5% of turnover in the pseudo-zero-order regime of catalysis (Figure 5).

These data show a first-order dependence on **[2]** and a half-order dependence on **[12]**. This is consistent with a rapid dimer/monomer equilibrium in which the dimer is dominant but sits off the cycle and a monomer is the active species. Such equilibria have been suggested before for arene



Scheme 11. Synthesis and reactivity of complex **12**. $[\text{BARF}_4]^-$ anions are not shown.



Scheme 12. Suggested relationships between **12** and **10**. (S) = solvent. $[\text{BARF}_4]^-$ anions are not shown.

alkylations,^[72] alkene hydrogenation^[65] and hydroboration,^[73] amine-borane dehydrogenation,^[58] C–S bond activations,^[74] and arylation of BCl-1,2-azaborines,^[75] amongst others. Perhaps most closely related to the system under discussion here are dimer/monomer equilibria operating for Shvo's catalyst in both amine-borane dehydrogenation and hydrogen transfer reactions.^[76,77] In these cases a dimer is suggested to be in equilibrium with two, different, monomers (of equal relative concentration); one of which is active in catalysis.

For the system here we speculate a rapid equilibrium is established between **12** and cationic (C) and neutral (D) monomers, for which one of the latter is the active catalyst (Scheme 13). We discount the alternative reason for half-order dependence that involves dissociation of either chelating phosphine or H_2 from **12**^[78] as this does not fit with other experimental observations. Reversible monomer/dimer equilibria for $[\text{Rh}(\text{L}_2)\text{H}_5]^+$ species involving reversible protonation have previously been noted,^[66,67] but we suggest that this is not occurring due to the positive effect that exogenous base has on the observed rate when starting from **10**, conditions that favour the formation of **12**. Consistent with the rapid equilibrium proposed, addition of MeCN (10 equivalents) to **12** resulted in the immediate formation of the monomeric MeCN-adduct **13** plus gas evolution (H_2), which could arise from C. Also formed are uncharacterised hydride products [^1H NMR: $\delta = -11.79$ and -17.45 ppm] that decompose after 1 h, suggestive of a reactive neutral species such as D.

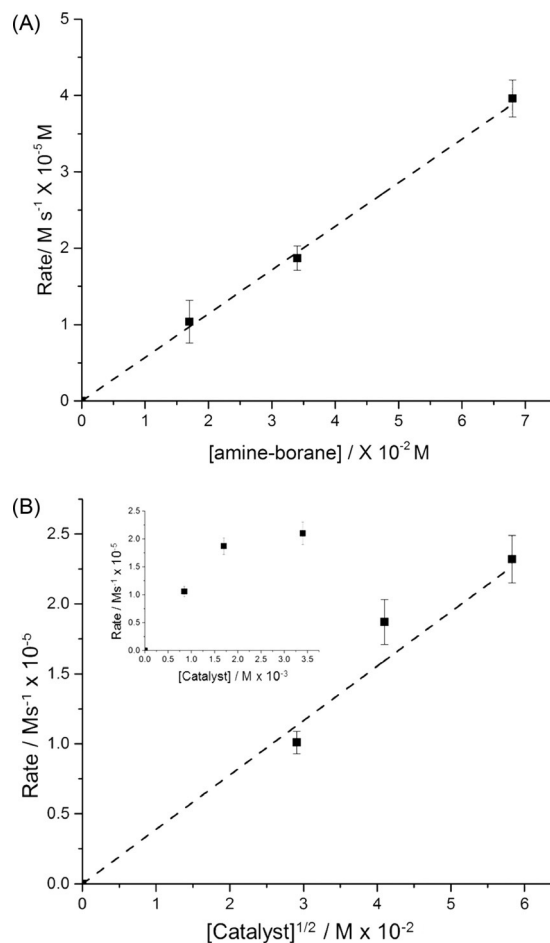
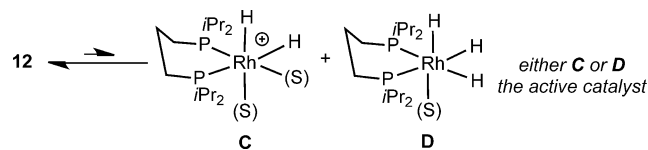


Figure 5. Initial rate versus concentration for the dehydrogenation of **2** mediated by **12** in a sealed NMR tube. A) $[\text{2}]$; B) $[\text{12}]^{1/2}$, inset shows relation to $[\text{12}]^1$.



Scheme 13. Suggested dimer/monomer equilibrium for **12**. $[\text{BARF}_4]^-$ anions are not shown. (S) = weakly bound solvent.

Conclusion

Presented here is the first study of the coordination chemistry, and subsequent dehydrogenation, of BN-cyclohexanes. Perhaps unsurprisingly the sigma-amine borane complexes formed with the $[\text{Ir}(\text{PCy}_3)_2(\text{H})_2]^+$ and $[\text{Rh}(\text{P}i\text{Pr}_2(\text{CH}_2)_3\text{P}i\text{Pr}_2)]^+$ fragments are broadly similar to those that result from coordination of acyclic amine-boranes, such as $\text{H}_3\text{B-NMe}_3$, although there are interesting differences in reactivity (e.g., the more levelled B–H/N–H activation energies when probed with exogenous D_2). The real insight that comes from these systems is their ability to mediate (albeit slowly) the dehydrogenation of the coordinated cyclic-amine boranes at room temperature that allows for intermediate species to be observed in the dehydrocoupling of the parent 2,2- H_2 -1,2-B,N- C_6H_{10} ; as well as (for the Rh system) the kinetics of dehydrogenation to be probed, which show half-order behaviour for the catalyst, suggesting a rapid dimer–monomer equilibrium is operating. Such insight is valuable in both determining dehydrocoupling pathways of cyclic amine-boranes and determining the speciation of the active catalyst species.

Experimental Section

All manipulations were performed under an argon atmosphere using standard Schlenk and glove-box techniques. Glassware was oven dried at 130°C , overnight, and flamed under vacuum prior to use. Pentane and MeCN were dried using a Grubbs-type solvent purification system (MBraun SPS-800) and degassed by successive freeze-pump-thaw cycles.^[79] $\text{C}_6\text{H}_5\text{F}$ and 1,2- $\text{F}_2\text{C}_6\text{H}_4$ were dried over CaH_2 , vacuum distilled and stored over 3 Å molecular sieves. $[\text{IrHP-Cy}_2(\eta^2\text{-C}_6\text{H}_9)\text{PCy}_2(\eta^3\text{-C}_6\text{H}_8)][\text{BAR}^{\text{F}}_4]$,^[16] $[\text{Rh}(\text{P}i\text{Pr}_2(\text{CH}_2)_3\text{P}i\text{Pr}_2)(\text{C}_6\text{H}_5\text{F})][\text{BAR}^{\text{F}}_4]$,^[62] $\text{Na}[\text{BAR}^{\text{F}}_4]$,^[80] $\text{Rh}(\text{P}i\text{Pr}_2(\text{CH}_2)_3\text{P}i\text{Pr}_2)_2(\mu\text{-H})_2$ ^[65] and $[\text{H}(\text{OEt})_2][\text{BAR}^{\text{F}}_4]$ ^[64] were prepared by literature methods. BN-cyclohexane (**1**), was prepared as described by Luo et al.^[9] NMR spectra were recorded on a Bruker AVIII-500 spectrometer at room temperature, or a Varian Unity/Inova 300 spectrometer 500 spectrometer. In $\text{C}_6\text{H}_5\text{F}$ and 1,2- $\text{C}_6\text{H}_4\text{F}_2$ solvents ^1H NMR spectra were referenced to the centre of the downfield solvent multiplet, $\delta = 7.11$ and 7.07 ppm, respectively. ^{31}P and ^{11}B NMR spectra were referenced against 85% H_3PO_4 (external) and $\text{BF}_3\cdot\text{OEt}_2$ (external), respectively. The spectrometer was pre-locked and pre-shimmed to the solvent mixture of 0.3 mL of 1,2- $\text{C}_6\text{H}_4\text{F}_2$ and 0.1 mL of C_6D_6 . Chemical shifts (δ) are quoted in ppm and coupling constants (J) in Hz. ESI-MS were recorded on a Bruker micrOTOF instrument interfaced with a glove-box.^[81] Electron impact high-resolution mass spectrometry (EI-HRMS) was performed at the Mass Spectrometry Facilities and Services Core of the Environmental Health Sciences Center at Oregon State University. Microanalysis was performed by Elemental Microanalysis Ltd. For hydrogenation reactions a high pressure NMR tube equipped with a J. Young's valve and the dissolved compound of interest was cooled to 77 K. The tube was evacuated and H_2 admitted (1 atm). The tube was sealed and warmed to 298 K, resulting in a pressure of approximately 4 atm ($298/77 \approx 4$).

Synthesis and characterization

N-Methyl-1,2-azaborinane 2: *B*-Cl-*N*-Me-1,2-BN-cyclohexene was prepared as described by Chrostowska and Liu.^[82] In a glovebox, a Fischer–Porter tube was charged with the starting material (4.00 g, 30.5 mmol) and palladium on carbon (64 mg, 10 wt % Pd

metal, 0.061 mmol, 0.2 mol% palladium). The vessel was sealed and flushed with hydrogen before pressurizing to 45 psi with hydrogen. The reaction was heated for 16 h with monitoring of the internal pressure and refilling as often as required. The reaction was then cooled to room temperature, and the solids were filtered off giving 1.68 g crude product (41% crude yield, 12.8 mmol). This crude product was dissolved in THF, and lithium aluminum hydride (1.12 g, 29.5 mmol, 2.3 equiv) was added carefully at room temperature. The reaction was stirred for 24 h at room temperature, and the solids were filtered off in the glovebox. The filtrate was cooled to -78°C , and methanol (10 mL) was added dropwise to quench excess LiAlH_4 and to install the proton on the product. The reaction was warmed to room temperature over 30 min, and the volatiles were removed in vacuo. The residue was extracted with hexane (4×80 mL), and the hexane was removed using a rotary evaporator. This residue was rinsed with cold pentane to furnish 374 mg of desired product (12% yield overall). ^1H NMR (500 MHz, C_6D_6): $\delta = 2.93$ – 2.07 (m, B-H signals), 1.93 (m, 3H), 1.72 (brs, 3H), 1.54 (brs, 2H), 1.35 (brs, 1H), 1.23 (brs, 1H), 0.87 (brs, 1H), 0.59 ppm (brs, 1H); ^{13}C NMR (126 MHz, C_6D_6): $\delta = 55.1$, 42.4, 28.8, 26.2, 16.6 ppm (br); ^{11}B NMR (96 MHz, C_6D_6): $\delta = -6.5$ ppm (t, $J(\text{BH}) = 96.4$ Hz); HRMS (EI+): m/z calcd for $\text{C}_5\text{H}_{13}\text{NB}$ [M]⁺ 98.114105, found 98.114265.

N,N-Dimethyl-1,2-azaborinane 3: The preparation of this compound was adapted from that of Wille and Goubeau.^[30] In a glovebox, a 300 mL pressure vessel was charged with tetrahydrofuran (100 mL) and *N,N*-dimethylhomoaallylamine (3.00 g, 30.3 mmol, 1 equiv). Borane-tetrahydrofuran solution (36 mL, 1 M in THF, 36 mmol, 1.2 equiv) was added dropwise. The pressure vessel was sealed, and the reaction was heated to 100°C for 18 h. The reaction was cooled to room temperature then opened in the air. The volatiles were removed in vacuo. The resulting residue, a viscous, colourless liquid, was subjected to silica gel chromatography in the air with 2:3 CH_2Cl_2 /hexane as the eluent system to furnish a colourless, viscous liquid (102 mg, 3%). ^1H NMR (300 MHz, C_6D_6): $\delta = 2.96$ – 2.13 (m, overlapping B-H signals), 2.06 (app t, 2H), 1.95 (s, 6H), 1.76 (brs 2H), 1.34–1.16 (m, 2H), 0.92 (brs, 2H). ^{13}C NMR (126 MHz, C_6D_6): $\delta = 62.4$, 50.3, 26.4, 25.0, 14.8 (br). ^{11}B NMR (96 MHz, C_6D_6): $\delta = -3.0$ (t, $J = 96.8$ Hz). HRMS (EI+) m/z calcd for $\text{C}_6\text{H}_{15}\text{NB}$ [M]⁺ 112.12976, found 112.12923.

$[\text{Ir}(\text{H}_2(\text{PCy}_3)_2(\eta^2\eta^2\text{-H}_2\text{BNH}_2(\text{CH}_2)_4))][\text{BAR}^{\text{F}}_4]$ (4): In a Young's flask, $[\text{IrHPCy}_2(\eta^2\text{-C}_6\text{H}_9)\text{PCy}_2(\eta^3\text{-C}_6\text{H}_8)][\text{BAR}^{\text{F}}_4]$ (44 mg, 2.7×10^{-2} mmol) in $\text{C}_6\text{H}_5\text{F}$ was hydrogenated at 4 atm as described in the general procedures. It was stirred for 20 min to produce a colourless solution of $[\text{Ir}(\text{H}_2(\text{PCy}_3)_2(\text{H}_2))][\text{BAR}^{\text{F}}_4]$ which was rapidly transferred under argon to a Schlenk flask containing **1** (2.3 mg, 2.7×10^{-2} mmol). The resulting colourless solution was stirred for 2 min at 25°C , then layered with pentane and held at -30°C for 72 h to afford the product as colourless crystal. Yield: 20 mg, 43%. ^1H NMR (500 MHz, CD_2Cl_2): $\delta = 7.76$ (s, 8H, $[\text{BAR}^{\text{F}}_4]^-$), 7.60 (s, 4H, $[\text{BAR}^{\text{F}}_4]^-$), 4.07 (br, 2H, NH_2), 3.23 (br, 2H, CH_2 next to NH_2), 1.93–1.4 (m, 35H, PCy_3 (33H) and CH_2 (2H)), 1.36–1.29 (m, 33H, PCy_3), 0.92 (m, 4H, CH_2), -6.23 (br, 2H, BH_2), -20.53 ppm (t, $^2J_{\text{HP}} = 16$ Hz, IrH_2). The NH_2/CH_2 resonances were identified on the basis of the number of cross-peaks in the $^1\text{H}/^1\text{H}$ COSY spectrum. Furthermore the HSQC spectrum shows no cross peak between the signal at $\delta = 4.07$ ppm, while the signal at $\delta = 3.23$ ppm is coupled to a ^{13}C NMR signal at 48 ppm. $^{31}\text{P}\{^1\text{H}\}$ NMR (202 MHz, CD_2Cl_2): $\delta = 37.12$ (d, $^2J_{\text{PP}} = 268$ Hz, 1P), 35.26 ppm (d, $^2J_{\text{PP}} = 268$ Hz, 1P); ^{11}B NMR (160 MHz, CD_2Cl_2): $\delta = 19.8$ (br, bound BH_2), -6.63 ppm (s, $[\text{BAR}^{\text{F}}_4]^-$); ESI-MS (1,2- $\text{C}_6\text{H}_4\text{F}_2$, 60°C) positive ion: m/z 840.5431 [M +] (calcd 840.5492); elemental microanalysis: calcd $[\text{C}_{72}\text{H}_{92}\text{B}_2\text{F}_{24}\text{IrNP}_2]$

(1703.28 g mol⁻¹): C 50.77, H 5.44, N 0.82; found: C 50.32, H 5.33, N 1.03.

[Ir(H)₂(PCy₃)₂(η²-H₂BNMeH(CH₂)₄)] [BAR^F₄] (5): In a high pressure NMR tube equipped with a J. Young's valve, [IrHPCy₂(η²-C₆H₆)PCy₂(η³-C₆H₈)] [BAR^F₄] (16 mg, 1 × 10⁻² mmol) in C₆H₅F was hydrogenated at 4 atm as described in the general procedures. It was stirred for 20 min to produce a colourless solution of [Ir(H)₂(PCy₃)₂(H₂)₂] [BAR^F₄] which was rapidly transferred under argon to another high pressure NMR tube containing **2** (1 mg, 1 × 10⁻² mmol). Gentle inversion of NMR tube for 1.5 h resulted in the colourless solution of **5** and Ir(H₂)(PCy₃)₂ in 20:1 ratio. Compound **5** was characterized in situ by NMR spectroscopy and ESI-MS. A few single crystals suitable for X-ray diffraction studies was obtained by diffusion of pentane at -35 °C. ¹H NMR (500 MHz, C₆H₅F): δ = 8.34 (s, 8H, [BAR^F₄]⁻), 7.67 (s, 4H, [BAR^F₄]⁻), 4.01 (br, 1H, NH), 3.13 (m, 1H, CH₂), 2.69 (m, 1H, CH₂), 2.46 (s, 3H, NMe), 1.93-1.56 (m, 37H, PCy₃ (33H) and CH₂ (4H)), 1.39-1.21 (m, 33H, PCy₃), 0.87 (m, 1H, CH₂), 0.67 (br, 1H, CH₂), -6.24 (br, 1H, BH₂), -6.35 (br, 1H, BH₂), -20.58 (br, 1H, IrH₂), -20.82 ppm (br, 1H, IrH₂); ³¹P{¹H} NMR (202 MHz, C₆H₅F): δ = 36.47 (d, ²J_{pp} = 276 Hz, 1P), 33.22 ppm (d, ²J_{pp} = 276 Hz, 1P); ¹¹B NMR (160 MHz, C₆H₅F): δ = 22.4 (br, bound BH₂), -6.10 ppm (s, [BAR^F₄]⁻); ESI-MS (1,2-C₆H₄F₂, 60 °C) positive ion: *m/z* 854.5533 [M⁺] (calcd 854.5649).

N-Methyl-1,2-azaborinene 8: This material has been reported by Wille and Goubeau, who invoke the intermediacy of the amino-borane **2** (which was not isolated in their study). Their procedure has been adapted here. *N*-Methylhomoallylamine (6.63 g, 77.9 mmol, 1 equiv) was cooled to 0 °C in 30 mL ether. Borane-tetrahydrofuran solution (0.9 M in THF, 103 mL, 93.4 mmol, 1.2 equiv) was added slowly via cannula. After the addition was completed, the ice bath was removed and the reaction was allowed to warm for 20 min before the solvent was removed in vacuo. The clear, colourless residue was rinsed with pentane (3 × 50 mL) in a glovebox, and the remaining insoluble residue was dissolved in benzene and heated to reflux (90 °C) for 24 h. After cooling to room temperature, the benzene solvent was distilled off under N₂, and the residue was submitted to vacuum transfer to a liquid nitrogen-cooled Schlenk flask. This procedure yielded 325 mg of a 1.25:1 molar ratio mixture of product/benzene (2% yield assuming equal density of benzene and product). ¹H NMR (300 MHz, CD₂Cl₂): δ = 2.92–2.80 (m, 5H, overlapping large singlet), 1.73–1.62 (m, 2H), 1.49–1.37 (m, 2H), 0.84 (brs, 2H) B-H proton visible at 5.0–3.75 ppm (q, 1H); ¹¹B NMR (96 MHz, CD₂Cl₂): δ = 40.62 ppm (d, *J* = 125 Hz); ¹H NMR (300 MHz, CD₂Cl₂): δ = 2.85 (m, overlapping with a singlet 5H), 1.66 (m, 2H), 1.44 (m, 2H), 0.84 ppm (m, 2H); ¹¹B NMR (97 MHz, CD₂Cl₂): δ = 40.0 ppm (d, *J* = 125 Hz).

[Rh(PiPr₂(CH₂)₃PiPr₂)(η²-H₂BNH₂C₄H₈)] [BAR^F₄] (9): 1,2-F₂C₆H₄ (0.5 mL) was added to a high-pressure NMR tube equipped with a J. Young's valve and charged with compound **1** (1.2 mg, 1.4 × 10⁻² mmol, 1.2 equivalents) and **V** (16 mg, 1.2 × 10⁻² mmol). Gentle rotation of NMR tube for 30 min resulted in reddish orange solution consisting of **9**, amino-borane **7** and **V** as measured by NMR spectroscopy. Compound **9** was characterized in situ by NMR spectroscopy and ESI-MS. Diffusion of pentane at -35 °C gave mixture of crystals corresponding to **9** (red) and **V** (orange). Red crystals were mechanically separated from orange crystals for single crystal X-ray diffraction studies. ¹H NMR (500 MHz, 1,2-C₆H₄F₂): δ = 8.33 (s, 8H, [BAR^F₄]⁻), 7.69 (s, 4H, [BAR^F₄]⁻), 4.54 (m, NH₂), 3.28 (br, CH₂), 3.18 (br, CH₂), 2.99 (br, CH₂), 1.76 (m, CH), 1.23–1.16 (m, CH₃), 1.06 (br, CH₂CH₂CH₂), -4.83 ppm (br, BH₂); ³¹P{¹H} NMR (202 MHz, 1,2-C₆H₄F₂): δ = 57.08 ppm (d, *J*_{RhP} = 160 Hz); ¹¹B NMR (160 MHz, 1,2-C₆H₄F₂): δ = 29.3 (br, BH₂), -6.19 ppm (s, [BAR^F₄]⁻); ESI-MS (1,2-C₆H₄F₂, 60 °C) positive ion: *m/z* 464.2284 [M⁺] (calcd 464.2248).

[Rh(iPr₂PCH₂CH₂CH₂PiPr₂)(η²-H₂BNHMeC₄H₈)] [BAR^F₄] (10): 1,2-F₂C₆H₄ (0.5 mL) was added to a Young's flask charged with **2** (4.5 mg, 4.5 × 10⁻², 2.5 equivalent) and **V** (25 mg, 1.8 × 10⁻² mmol). The resulting orange solution was stirred for 30 min to obtain a red solution. Diffusion of pentane into this solution at -35 °C for 72 h afforded **10** as red crystals. Yield: 10 mg, 41%. ¹H NMR (500 MHz, CD₂Cl₂): δ = 7.76 (s, 8H, [BAR^F₄]⁻), 7.60 (s, 4H, [BAR^F₄]⁻), 3.94 (br, 1H, NH), 3.33 (br d, 1H, CH₂), 2.91 (d, ³J_{HH} = 5 Hz, 3H, NMe), 2.76 (m, 1H, CH₂), 2.37 (br, 1H, CH₂), 1.99–1.92 (br, 6H, CH (4H) and CH₂ (2H)), 1.65 (m, 1H, CH₂), 1.5–1.0 (br m, 26H, CH₃ (24H) and CH₂ (2H)), 0.52 (br, CH₂CH₂CH₂), -4.9 (br, 1H, BH₂), -5.38 ppm (br, 1H, BH₂); ³¹P{¹H} NMR (202 MHz, CD₂Cl₂): δ = 57.87 ppm (d, *J*_{RhP} = 162 Hz); ³¹P{¹H} NMR (202 MHz, CD₂Cl₂, 190 K): δ = 57.75 (overlapping dd, 1P, *J*_{RhP} = 160 Hz, *J*_{pp} = 56 Hz), 56.85 ppm (overlapping dd, 1P, *J*_{RhP} = 160 Hz, *J*_{pp} = 56 Hz); ¹¹B NMR (160 MHz, CD₂Cl₂): δ = 32.1 (br, BH₂), -6.60 ppm (s, [BAR^F₄]⁻); ESI-MS (1,2-C₆H₄F₂, 60 °C) positive ion: *m/z* 478.2417 [M⁺] (calcd 478.2408); elemental microanalysis: calcd [C₅₂H₆₀B₂F₂₄NP₂Rh] (1341.49 g mol⁻¹): C 46.56, H 4.51, N 1.04; found: C 46.17, H 4.16, N 0.68.

[Rh(iPr₂PCH₂CH₂CH₂PiPr₂)(η²-H₂BNMe₂C₄H₈)] [BAR^F₄] (11): To a high pressure NMR tube equipped with a J. Young's valve and charged with **3** (0.69 mmol in 1,2-F₂C₆H₄, 0.04 mL, 2.6 × 10⁻² mmol, 2 equivalent) and **V** (18 mg, 1.3 × 10⁻² mmol) was added 1,2-F₂C₆H₄ (0.4 mL). The NMR tube was gently inverted at 25 °C and the reaction was followed by periodic NMR spectroscopy. After 24 h the reaction was complete and the resulting red solution was layered with pentane and kept at 25 °C for 72 h to afford the product as red crystals. Yield: 8 mg, 45%. ¹H NMR (500 MHz, CD₂Cl₂): δ = 7.76 (s, 8H, [BAR^F₄]⁻), 7.60 (s, 4H, [BAR^F₄]⁻), 2.99 (br, 2H, CH₂), 2.85 (s, 6H, NMe₂), 1.92 (m, 4H, CH), 1.79 (br, 2H, CH₂), 1.65 (br, 2H, CH₂), 1.50 (br, 2H, CH₂), 1.23 (br, 24H, CH₃), 0.5 (br, 6H, CH₂CH₂CH₂), -5.17 ppm (br, 2H, BH₂); ³¹P{¹H} NMR (202 MHz, CD₂Cl₂): δ = 58.03 ppm (d, *J*_{RhP} = 163 Hz); ¹¹B NMR (160 MHz, CD₂Cl₂): δ = 34.4 (br, BH₂), -6.6 ppm (s, [BAR^F₄]⁻); ESI-MS (1,2-C₆H₄F₂, 60 °C) positive ion: *m/z* 492.2548 [M⁺] (calcd 492.2565); elemental microanalysis: calcd [C₅₃H₆₂B₂F₂₄NP₂Rh] (1355.52 g mol⁻¹): C 46.96, H 4.61, N 1.03; found: C 46.65, H 4.10, N 0.62.

[[Rh(PiPr₂(CH₂)₃PiPr₂)₂(H)₂(μ-H)₃]] [BAR^F₄] (12): [Rh(PiPr₂(CH₂)₃PiPr₂)₂(μ-H)₂] (23 mg, 0.03 mmol) and [H(OEt)₂] [BAR^F₄] (30 mg, 0.03 mmol) were added to a Young's flask. Addition of 1 mL of 1,2-F₂C₆H₄ led to the formation of a dark red solution which was immediately hydrogenated at 4 atm as described in the general procedures. The resulting solution was stirred for 1 h to obtain a dark orange solution. The solution was filtered into a crystallisation tube, layered with pentane and kept at -18 °C for 24 h from which dark red crystals were obtained in 70% yield (34 mg). This complex decomposes in CH₂Cl₂ solution (12 h) to give unidentified products, but shows greater stability in 1,2-F₂C₆H₄ (no decomposition after 24 h). See the Supporting Information for a solid-state structure as determined by single crystal X-ray diffraction. ¹H NMR (400 MHz, CD₂Cl₂): δ = 7.76 (s, 8H, [BAR^F₄]⁻), 7.60 (s, 4H, [BAR^F₄]⁻), 1.96 (m, 8H, CH), 1.56–1.1 (m, 60H, CH₃ (48H) and CH₂ (12H)), -8.85 (br, 3H), -18.87 ppm (br, 2H); ¹H NMR (500 MHz, 1,2-C₆H₄F₂): δ = 8.34 (s, 8H, [BAR^F₄]⁻), 7.70 (s, 4H, [BAR^F₄]⁻), 1.96 (m, 8H, CH), 1.55–1.11 (m, 60H, CH₃ (48H) and CH₂ (12H)), -8.25 (br, 3H), -18.90 ppm (br, 2H); ¹H NMR (500 MHz, 1,2-C₆H₄F₂, 250 K): δ = 8.34 (s, 8H, [BAR^F₄]⁻), 1.93 (m, 8H, CH), 1.40–0.91 (m, 60H, CH₃ (48H) and CH₂ (12H)), -7.91 (br, 2H), -9.52 (br, 1H), -18.71 ppm (br, 2H); ³¹P{¹H} NMR (162 MHz, CD₂Cl₂): δ = 65.71 (br), 62.68 ppm (br); ³¹P{¹H} NMR (202 MHz, 1,2-C₆H₄F₂): δ = 66.49 (br), 62.22 (br). ³¹P{¹H} NMR (202 MHz, 1,2-C₆H₄F₂, 250 K): δ = 66.36 (br d, *J*_{RhP} = 100 Hz), 60.00 ppm (br d, *J*_{RhP} = 100 Hz); ¹¹B NMR (128 MHz, CD₂Cl₂): δ = -6.63 ppm (s, [BAR^F₄]⁻); ¹¹B NMR (160 MHz, 1,2-C₆H₄F₂): δ =

–6.19 ppm (s, [BAR^F₄][–]); elemental microanalysis: calcd [C₆₂H₈₅BF₂₄P₄Rh₂] (1626.34 g mol^{–1}): C 45.77, H 5.27; found: C 45.33, H 4.84.

[Rh(*i*Pr₂P(CH₂)₃P*i*Pr₂)(NCMe)₂][BAR^F₄] (**13**): **V** (20 mg, 1.4 × 10^{–2} mmol) was dissolved in 1,2-F₂C₆H₄ (1 mL) in a Schlenk flask to which CH₃CN (16 μL, 0.28 mmol, 20 equivalents) was added. Addition of CH₃CN immediately changed the colour of solution from orange to pale yellow. Resulting solution was stirred for 10 min. 1,2-F₂C₆H₄ and unreacted CH₃CN were removed in vacuo to obtain pale yellow solid of **13**. Yield: 14 mg, 70%. ¹H NMR (500 MHz, CD₂Cl₂): δ = 7.76 (s, 8H, [BAR^F₄][–]), 7.61 (s, 4H, [BAR^F₄][–]), 2.25 (s, 6H, NCCH₃), 1.97 (br, 6H, CH₂), 1.33 (m, 16H, CH₃ (12H) and CH (4H)), 1.19 ppm (m, 12H, CH₃); ³¹P{¹H} NMR (202 MHz, CD₂Cl₂): δ = 42.51 ppm (d, *J*_{RhP} = 167 Hz); ESI-MS (1,2-C₆H₄F₂, 60 °C) positive ion: *m/z* 461.1748 [*M*⁺] (calcd 461.1722); elemental microanalysis: calcd [C₅₁H₅₂BF₂₄N₂P₂Rh] (1324.62 g mol^{–1}): C 46.24, H 3.96, N 2.11; found: C 46.13, H 3.95, N 1.98.

Computational Methods

The geometries were optimized at the density functional theory (DFT)^[83] level with the hybrid B3LYP^[84,85] exchange-correlation functional and the DFT-optimized DZVP2 basis set for all atoms.^[86] Vibrational frequencies were calculated to show that the structures were minima. The nuclear magnetic shielding tensors were calculated using the gauge-independent atomic orbital (GIAO) approach.^[87,88] The NMR calculations were carried out with the TZVP basis set and B3LYP exchange-correlation functional.^[89] All calculations were carried out with Gaussian 09.^[90]

Acknowledgements

The Rhodes Trust (A.K.) and the EPSRC (EP/M024210, EP/J02127X) are thanked for support. Financial support was also provided in part by the National Institute of Environmental Health Sciences, NIH (P30 ES00210); S.-Y.L. and D.A.D. thank the US Department of Energy (DE-EE-0005658) for financial support and the Camille Dreyfus Teacher–Scholar Awards Program. D.A.D. thanks the Robert Ramsay Chair Fund of The University of Alabama for support. J.S.A.I. thanks the LaMattina Family Graduate Fellowship in Chemical Synthesis for support and Mr. Z. X. Giustra and Dr. P. G. Campbell for helpful discussions regarding synthesis of cyclic amine-boranes.

Keywords: amine-borane • catalysis • iridium • phosphine • rhodium

- [1] H. C. Johnson, T. N. Hooper, A. S. Weller, *Top. Organomet. Chem.* **2015**, *49*, 153.
- [2] E. M. Leitao, T. Jurca, I. Manners, *Nat. Chem.* **2013**, *5*, 817.
- [3] A. Staubitz, A. P. M. Robertson, M. E. Sloan, I. Manners, *Chem. Rev.* **2010**, *110*, 4023.
- [4] N. E. Stubbs, A. P. M. Robertson, E. M. Leitao, I. Manners, *J. Organomet. Chem.* **2013**, *730*, 84.
- [5] R. Waterman, *Chem. Soc. Rev.* **2013**, *42*, 5629.
- [6] C. W. Hamilton, R. T. Baker, A. Staubitz, I. Manners, *Chem. Soc. Rev.* **2009**, *38*, 279.
- [7] P. G. Campbell, A. J. V. Marwitz, S.-Y. Liu, *Angew. Chem. Int. Ed.* **2012**, *51*, 6074; *Angew. Chem.* **2012**, *124*, 6178.
- [8] P. G. Campbell, L. N. Zakharov, D. J. Grant, D. A. Dixon, S.-Y. Liu, *J. Am. Chem. Soc.* **2010**, *132*, 3289.
- [9] W. Luo, L. N. Zakharov, S.-Y. Liu, *J. Am. Chem. Soc.* **2011**, *133*, 13006.

- [10] W. Luo, P. G. Campbell, L. N. Zakharov, S.-Y. Liu, *J. Am. Chem. Soc.* **2011**, *133*, 19326.
- [11] W. Luo, D. Neiner, A. Karkamkar, K. Parab, E. B. Garner, D. A. Dixon, D. Matson, T. Autrey, S.-Y. Liu, *Dalton Trans.* **2013**, *42*, 611.
- [12] G. Chen, L. N. Zakharov, M. E. Bowden, A. J. Karkamkar, S. M. Whittemore, E. B. Garner, T. C. Mikulas, D. A. Dixon, T. Autrey, S.-Y. Liu, *J. Am. Chem. Soc.* **2015**, *137*, 134.
- [13] P. G. Campbell, J. S. A. Ishibashi, L. N. Zakharov, S.-Y. Liu, *Aust. J. Chem.* **2014**, *67*, 521.
- [14] M. Shimoi, S. Nagai, M. Ichikawa, Y. Kawano, K. Katoh, M. Uruichi, H. Ogino, *J. Am. Chem. Soc.* **1999**, *121*, 11704.
- [15] G. J. Kubas, *Metal Dihydrogen and σ-Bond Complexes*, Kluwer, New York, **2001**.
- [16] G. Alcaraz, A. B. Chaplin, C. J. Stevens, E. Clot, L. Vendier, A. S. Weller, S. Sabo-Etienne, *Organometallics* **2010**, *29*, 5591.
- [17] C. J. Stevens, R. Dallanegra, A. B. Chaplin, A. S. Weller, S. A. Macgregor, B. Ward, D. Mckay, G. Alcaraz, S. Sabo-Etienne, *Chem. Eur. J.* **2011**, *17*, 3011.
- [18] A. Kumar, H. C. Johnson, T. N. Hooper, A. S. Weller, A. G. Algarra, S. A. Macgregor, *Chem. Sci.* **2014**, *5*, 2546.
- [19] R. Dallanegra, A. P. M. Robertson, A. B. Chaplin, I. Manners, A. S. Weller, *Chem. Commun.* **2011**, *47*, 3763.
- [20] H. C. Johnson, E. M. Leitao, G. R. Whittell, I. Manners, G. C. Lloyd-Jones, A. S. Weller, *J. Am. Chem. Soc.* **2014**, *136*, 9078.
- [21] A. B. Chaplin, A. S. Weller, *Inorg. Chem.* **2010**, *49*, 1111.
- [22] R. Dallanegra, A. B. Chaplin, J. Tsim, A. S. Weller, *Chem. Commun.* **2010**, *46*, 3092.
- [23] C. J. Wallis, H. Dyer, L. Vendier, G. Alcaraz, S. Sabo-Etienne, *Angew. Chem. Int. Ed.* **2012**, *51*, 3646; *Angew. Chem.* **2012**, *124*, 3706.
- [24] C. J. Wallis, G. Alcaraz, A. S. Petit, A. I. Poblador-Bahamonde, E. Clot, C. Bijani, L. Vendier, S. Sabo-Etienne, *Chem. Eur. J.* **2015**, *21*, 13080.
- [25] A. Wagner, E. Kaifer, H.-J. Himmel, *Chem. Commun.* **2012**, *48*, 5277.
- [26] A. Wagner, S. Litters, J. Elias, E. Kaifer, H.-J. Himmel, *Chem. Eur. J.* **2014**, *20*, 12514.
- [27] M. Hata, Y. Kawano, M. Shimoi, *Inorg. Chem.* **1998**, *37*, 4482.
- [28] F.-C. Liu, J. Liu, E. A. Meyers, S. G. Shore, *Inorg. Chem.* **1998**, *37*, 3293.
- [29] Wille has implicated amine-borane 2 as an intermediate in the synthesis of amino-borane **8**. See Ref. [30].
- [30] H. Wille, J. Goubeau, *Chem. Ber.* **1972**, *105*, 2156.
- [31] In this contribution we use the nomenclature η²η² to describe the bonding in two B–H...M 3c–2e interactions. However an alternative κ²-nomenclature is also possible: See: J. C. Green, M. L. H. Green, G. Parkin, *Chem. Commun.* **2012**, *48*, 11481.
- [32] G. Alcaraz, S. Sabo-Etienne, *Angew. Chem. Int. Ed.* **2010**, *49*, 7170; *Angew. Chem.* **2010**, *122*, 7326.
- [33] H. C. Johnson, A. P. M. Robertson, A. B. Chaplin, L. J. Sewell, A. L. Thompson, M. F. Haddow, I. Manners, A. S. Weller, *J. Am. Chem. Soc.* **2011**, *133*, 11076.
- [34] A. E. W. Ledger, C. E. Ellul, M. F. Mahon, J. M. J. Williams, M. K. Whittlesey, *Chem. Eur. J.* **2011**, *17*, 8704.
- [35] R. Dallanegra, A. B. Chaplin, A. S. Weller, *Angew. Chem. Int. Ed.* **2009**, *48*, 6875; *Angew. Chem.* **2009**, *121*, 7007.
- [36] A. B. Chaplin, A. S. Weller, *Angew. Chem. Int. Ed.* **2010**, *49*, 581; *Angew. Chem.* **2010**, *122*, 591.
- [37] M. O'Neill, D. A. Addy, I. Riddlestone, M. Kelly, N. Phillips, S. Aldridge, *J. Am. Chem. Soc.* **2011**, *133*, 11500.
- [38] G. Alcaraz, S. Sabo-Etienne, *Coord. Chem. Rev.* **2008**, *252*, 2395.
- [39] N. Merle, G. Koicok-Köhn, M. F. Mahon, C. G. Frost, G. D. Ruggiero, A. S. Weller, M. C. Willis, *Dalton Trans.* **2004**, 3883.
- [40] A. G. Algarra, L. J. Sewell, H. C. Johnson, S. A. Macgregor, A. S. Weller, *Dalton Trans.* **2014**, *43*, 11118.
- [41] K. Gruet, E. Clot, O. Eisenstein, D. H. Lee, B. Patel, A. Macchioni, R. H. Crabtree, *New J. Chem.* **2003**, *27*, 80.
- [42] H. C. Johnson, A. S. Weller, *J. Organomet. Chem.* **2012**, *721–722*, 17.
- [43] O. J. Metters, A. M. Chapman, A. P. M. Robertson, C. H. Woodall, P. J. Gates, D. F. Wass, I. Manners, *Chem. Commun.* **2014**, *50*, 12146.
- [44] E. M. Leitao, N. E. Stubbs, A. P. Robertson, H. Helten, R. J. Cox, G. C. Lloyd-Jones, I. Manners, *J. Am. Chem. Soc.* **2012**, *134*, 16805.
- [45] C. A. Jaska, K. Temple, A. J. Lough, I. Manners, *J. Am. Chem. Soc.* **2003**, *125*, 9424.

- [46] H. A. Kalviri, F. Gärtner, E. Ye, I. Korobkov, R. T. Baker, *Chem. Sci.* **2014**, *5*, 618.
- [47] X. Chen, J.-C. Zhao, S. G. Shore, *Acc. Chem. Res.* **2013**, *46*, 2666.
- [48] S. Aldridge, A. J. Downs, C. Y. Tang, S. Parsons, M. C. Clarke, R. D. L. Johnstone, H. E. Robertson, D. W. H. Rankin, D. A. Wann, *J. Am. Chem. Soc.* **2009**, *131*, 2231.
- [49] V. Butera, N. Russo, E. Sicilia, *ACS Catal.* **2014**, *4*, 1104.
- [50] M. T. Nguyen, V. S. Nguyen, M. H. Matus, G. Gopakumar, D. A. Dixon, *J. Phys. Chem. A* **2007**, *111*, 679.
- [51] V. S. Nguyen, M. H. Matus, D. J. Grant, M. T. Nguyen, D. A. Dixon, *J. Phys. Chem. A* **2007**, *111*, 8844.
- [52] Calculations at the G3MP2 level show that dehydrogenation to form **7** is exogonic by $-15.8 \text{ kcal mol}^{-1}$, suggesting reversible dehydrogenation is not occurring in the H/D exchange process. See: M. H. Matus, S.-Y. Liu, D. A. Dixon, *J. Phys. Chem. A* **2010**, *114*, 2644.
- [53] T. M. Douglas, A. B. Chaplin, A. S. Weller, X. Yang, M. B. Hall, *J. Am. Chem. Soc.* **2009**, *131*, 15440.
- [54] M. Parafiniuk, M. P. Mitoraj, *Organometallics* **2013**, *32*, 4103.
- [55] T. D. Forster, H. M. Tuononen, M. Parvez, R. Roesler, *J. Am. Chem. Soc.* **2009**, *131*, 6689.
- [56] H. Helten, B. Dutta, J. R. Vance, M. E. Sloan, M. F. Haddow, S. Sproules, D. Collison, G. R. Whittell, G. C. Lloyd-Jones, I. Manners, *Angew. Chem. Int. Ed.* **2013**, *52*, 437; *Angew. Chem.* **2013**, *125*, 455.
- [57] M. C. MacInnis, R. McDonald, M. J. Ferguson, S. Tobisch, L. Turculet, *J. Am. Chem. Soc.* **2011**, *133*, 13622.
- [58] L. J. Sewell, M. A. Huertos, M. E. Dickinson, A. S. Weller, G. C. Lloyd-Jones, *Inorg. Chem.* **2013**, *52*, 4509.
- [59] R. T. Baker, J. C. Gordon, C. W. Hamilton, N. J. Henson, P.-H. Lin, S. Maguire, M. Murugesu, B. L. Scott, N. C. Smythe, *J. Am. Chem. Soc.* **2012**, *134*, 5598.
- [60] Y. Jiang, O. Blacque, T. Fox, C. M. Frech, H. Berke, *Organometallics* **2009**, *28*, 5493.
- [61] M. A. Huertos, A. S. Weller, *Chem. Sci.* **2013**, *4*, 1881.
- [62] I. Pernik, J. F. Hooper, A. B. Chaplin, A. S. Weller, M. C. Willis, *ACS Catal.* **2012**, *2*, 2779.
- [63] A. S. Weller, T. P. Fehlner, *Organometallics* **1999**, *18*, 447.
- [64] M. Brookhart, B. Grant, A. F. Volpe, *Organometallics* **1992**, *11*, 3920.
- [65] M. D. Fryzuk, W. E. Piers, F. W. B. Einstein, T. Jones, *Can. J. Chem.* **1989**, *67*, 883.
- [66] I. R. Butler, W. R. Cullen, T.-J. Kim, F. W. B. Einstein, T. Jones, *J. Chem. Soc. Chem. Commun.* **1984**, 719.
- [67] C. Kohrt, W. Baumann, A. Spannenberg, H.-J. Drexler, I. D. Gridnev, D. Heller, *Chem. Eur. J.* **2013**, *19*, 7443.
- [68] J. Wolf, O. Nürnberg, M. Schäfer, H. Werner, *Z. Anorg. Allg. Chem.* **1994**, *620*, 1157.
- [69] M. Roselló-Merino, J. López-Serrano, S. Conejero, *J. Am. Chem. Soc.* **2013**, *135*, 10910.
- [70] L. J. Sewell, G. C. Lloyd-Jones, A. S. Weller, *J. Am. Chem. Soc.* **2012**, *134*, 3598.
- [71] H. C. Johnson, A. S. Weller, *Angew. Chem. Int. Ed.* **2015**, *54*, 10.1002; *Angew. Chem.* **2015**, *127*, 2/anie.201504073.
- [72] G. P. Van Strijdonck, M. D. Boele, P. C. Kamer, J. G. De Vries, P. van Leeuwen, *Eur. J. Inorg. Chem.* **1999**, 1073.
- [73] J. M. Brown, G. C. Lloyd-Jones, *J. Chem. Soc. Chem. Commun.* **1992**, 710.
- [74] J. F. Hooper, R. D. Young, I. Pernik, A. S. Weller, M. C. Willis, *Chem. Sci.* **2013**, *4*, 1568.
- [75] G. E. Rudebusch, L. N. Zakharov, S.-Y. Liu, *Angew. Chem. Int. Ed.* **2013**, *52*, 9316; *Angew. Chem.* **2013**, *125*, 9486.
- [76] J. B. Johnson, J.-E. Bäckvall, *J. Org. Chem.* **2003**, *68*, 7681.
- [77] Z. Lu, B. L. Conley, T. J. Williams, *Organometallics* **2012**, *31*, 6705.
- [78] J. E. Marshall, J. B. Keister, S. T. Diver, *Organometallics* **2011**, *30*, 1319.
- [79] A. B. Pangborn, M. A. Giardello, R. H. Grubbs, R. K. Rosen, F. J. Timmers, *Organometallics* **1996**, *15*, 1518.
- [80] W. E. Buschmann, J. S. Miller, *Inorg. Synth.* **2002**, *33*, 83.
- [81] A. T. Lubben, J. S. McIndoe, A. S. Weller, *Organometallics* **2008**, *27*, 3303.
- [82] A. Chrostowska, S. Xu, A. N. Lamm, A. Mazière, C. D. Weber, A. Dargelos, P. Baylère, A. Graciaa, S.-Y. Liu, *J. Am. Chem. Soc.* **2012**, *134*, 10279.
- [83] R. G. Parr, W. Yang, *Density-Functional Theory of Atoms and Molecules*, Oxford University Press, New York, **1989**.
- [84] A. D. Becke, *J. Chem. Phys.* **1993**, *98*, 5648.
- [85] C. Lee, W. Yang, R. G. Parr, *Phys. Rev. B* **1988**, *37*, 785.
- [86] N. Godbout, D. R. Salahub, J. Andzelm, E. Wimmer, *Can. J. Chem.* **1992**, *70*, 560.
- [87] K. Wolinski, J. F. Hinton, P. Pulay, *J. Am. Chem. Soc.* **1990**, *112*, 8251.
- [88] J. R. Cheeseman, G. W. Trucks, T. A. Keith, M. J. Frisch, *J. Chem. Phys.* **1996**, *104*, 5497.
- [89] A. Schäfer, H. Horn, R. Ahlrichs, *J. Chem. Phys.* **1992**, *97*, 2571.
- [90] Gaussian 09, Revision B.1, M. J. Frisch, G. W. Trucks, H. B. Schlegel, G. E. Scuseria, M. A. Robb, J. R. Cheeseman, G. Scalmani, V. Barone, B. Menonucci, G. A. Petersson, H. Nakatsuji, M. Caricato, X. Li, H. P. Hratchian, A. F. Izmaylov, J. Bloino, G. Zheng, J. L. Sonnenberg, M. Hada, M. Ehara, K. Toyota, R. Fukuda, J. Hasegawa, M. Ishida, T. Nakajima, Y. Honda, O. Kitao, H. Nakai, T. Vreven, J. A. Montgomery, Jr., J. E. Peralta, F. Ogliaro, M. Bearpark, J. J. Heyd, E. Brothers, K. N. Kudin, V. N. Staroverov, T. Keith, R. Kobayashi, J. Normand, K. Raghavachari, A. Rendell, J. C. Burant, S. S. Iyengar, J. Tomasi, M. Cossi, N. Rega, J. M. Millam, M. Klene, J. E. Knox, J. B. Cross, V. Bakken, C. Adamo, J. Jaramillo, R. Gomperts, R. E. Stratmann, O. Yazyev, A. J. Austin, R. Cammi, C. Pomelli, J. W. Ochterski, R. L. Martin, K. Morokuma, V. G. Zakrzewski, G. A. Voth, P. Salvador, J. J. Dannenberg, S. Dapprich, A. D. Daniels, O. Farkas, J. B. Foresman, J. V. Ortiz, J. Cioslowski, D. J. Fox, **2009**, Gaussian, Inc., Wallingford CT.

Received: July 30, 2015

Published online on November 25, 2015